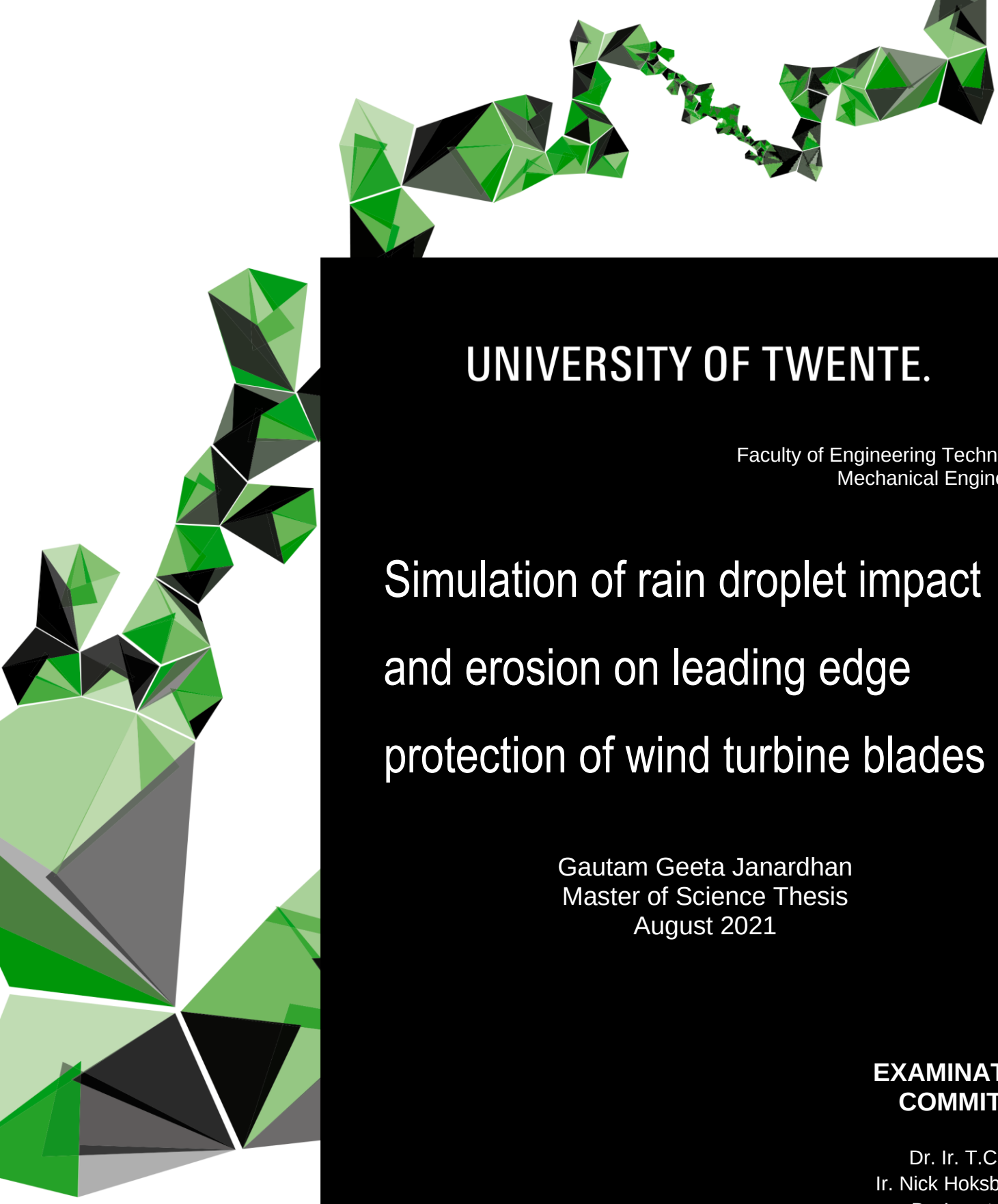

UNIVERSITY OF TWENTE.

Faculty of Engineering Technology,
Mechanical Engineering

Simulation of rain droplet impact and erosion on leading edge protection of wind turbine blades

Gautam Geeta Janardhan
Master of Science Thesis
August 2021

EXAMINATION COMMITTEE

Dr. Ir. T.C. BOR
Ir. Nick Hoksbergen
Dr. Ismet Baran
Dr. Javad Hazrati Marangalou

University of Twente
P.O. Box 217
7500 AE Enschede
The Netherlands

SUMMARY

Transitioning towards renewable energy, offshore wind farms show high potential amongst the renewable sources of energy. In efforts to maximize outputs, the dimensions of these wind turbines have increased. This resulted in higher tip speeds (more than 100m/s), which when combined with the interactions with rain droplets causes damage over time. The accelerated rates of erosion along the turbine adversely affects the performance of the wind turbine, which reduces the levelized cost of energy and annual energy production. To prevent erosion, protective coatings like leading edge protection (LEP) are implemented, however, the current solutions are not ideal as they fail to protect the turbines at higher speeds. Hence, a new optimized solution is required that can be adapted across the industry to prevent erosion of wind turbine blades.

This thesis studied the droplet-substrate interaction for different materials by modeling this fluid-structure interaction in Abaqus using a combination of Smoothed Particle Hydrodynamics (SPH) and Lagrangian methods. Thermoplastics are used to define the LEP which is co-bonded to an epoxy substrate across a discrete interface and a continuous interphase. To ensure comparability between the results, a standard model was developed to have a good resolution of the stress field while having a relatively low computational time. This model was then adapted to different LEP materials like TPU and ABS for the aforementioned simulations.

Studying the stress fields for the discrete and continuous interphases, the influence of LEP thickness on wave propagation through the system was studied. This was achieved by studying the response of pure polymeric materials for varying LEP thicknesses. Then the discrete interface was defined for an epoxy substrate and LEP using the standard model. The interfaces/interphases were varied and the stress fields were studied. From these stress fields, stress concentrations and possible damage locations were determined. This, combined with the geometric and material parameters of the system helped to establish the performance of the studied LEP materials. This thesis derives a set of design guidelines for an integrated LEP (InLEP) solution to prevent rain erosion in wind turbine blades.

Table of Contents

List of Figures

List of Tables

Chapter 1 : Introduction

The efforts to transition towards renewable energy to reduce energy dependency on fossil fuels and mitigate the adverse effects of climate change, have resulted in the setup of new wind farms. Of the renewable sources of energy available, wind energy shows high potential to meet the global energy demand, especially offshore wind farms. In 2020, Europe installed 14.7 GW of new wind power, 1.98 GW was produced by the Netherlands, 75% of which was from offshore wind power as shown in Figure 1 [1]. Wind farms help decarbonize the industry with long term agreements providing the energy required. In Europe, 16% of the energy demand is supplied with wind energy [2]. The projection for installed wind energy in the future is shown to increase in Europe as shown in Figure 2.

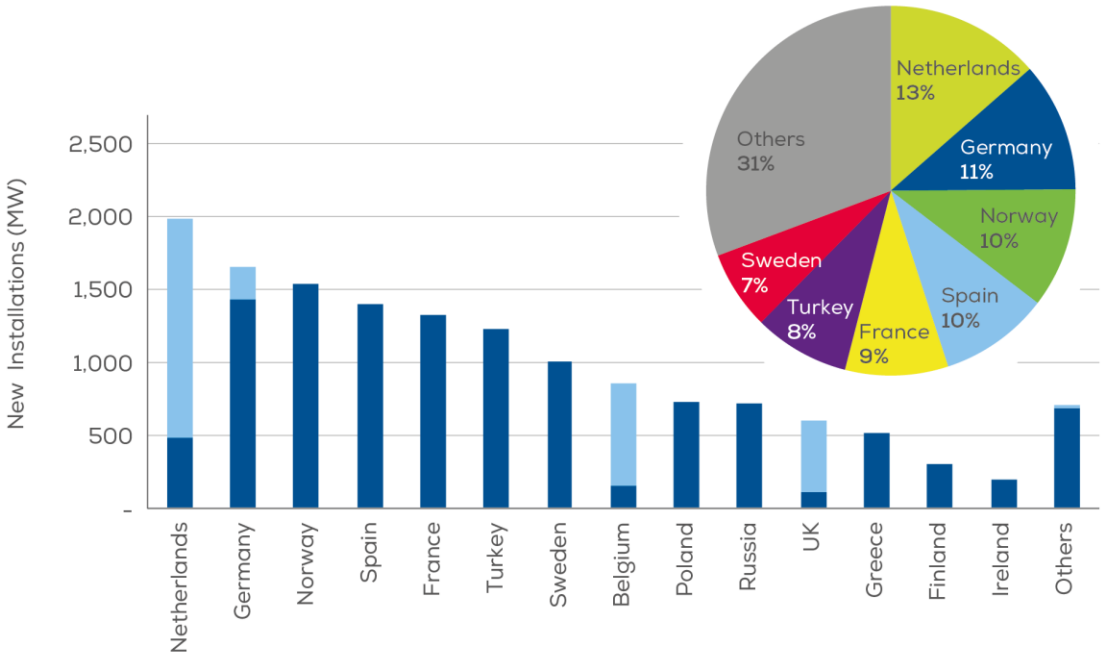

	Netherlands	Germany	Norway	Spain	France	Turkey	Sweden	Belgium	Poland	Russia	UK	Greece	Finland	Ireland	Others
Offshore	1,493	219	-	-	-	-	-	706	-	-	483	-	-	-	17
Onshore	486	1,431	1,532	1,400	1,318	1,224	1,007	152	731	713	115	517	302	196	688
Total	1,979	1,650	1,532	1,400	1,318	1,224	1,007	858	731	713	598	517	302	196	705

Figure 1. Newly installed wind power capacity in Europe in 2020 *[1]*.

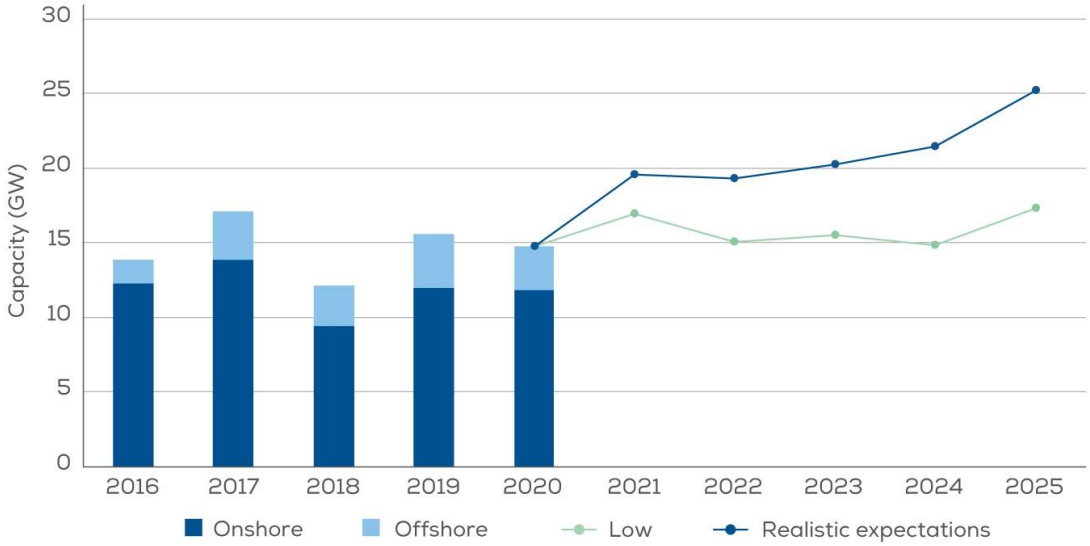

Figure 2. Installed wind power in Europe and projections for the future *[1]*.

Offshore wind farms have their own pros and cons compared to onshore wind farms. Offshore turbines can have larger dimensions as a typical wind turbine extracts approximately 50% of energy passing through the rotor area. In contrast, onshore wind farms experience less wind and need to be isolated from settlements to avoid noise pollution and therefore, have limitations on the turbine dimensions. New offshore projects have capacity factors of 40-50%, as larger turbines and technology improvements help to make most of the available wind energy [3]. However, as the wind turbines increase in size to capture more energy, the damage caused due to erosion also increases. Erosion due to atmospheric particles like rain, dust, hail, and snow, leads to surface roughness followed by increased aerodynamic drag in the blades which reduces the energy output, thus, adversely affecting the performance and life of the wind turbine [4]. A characteristic form of this erosion observed in wind turbine blades is called the Leading-Edge Erosion. Research is being carried out to understand this erosion in detail and develop suitable preventive mechanisms to improve blade performance.

1.1 Literature Review

Wind turbine blades are critical components of the wind turbine and are typically built from glass fiber reinforced polymer composites to achieve suitable mechanical properties while being lightweight. This results in the turbine blade undergoing different failure modes compared to alloys or metals, such as delamination, debonding, and cracks and cratering on the surface, as shown in Figure 3. This affects the performance and output of the wind turbine, which reduces the levelized cost of energy and annual energy production (AEP). Additionally, other factors such as manufacturing, transportation and installation may result in surface damage that serve as points of erosion initiation in the wind turbine [5].

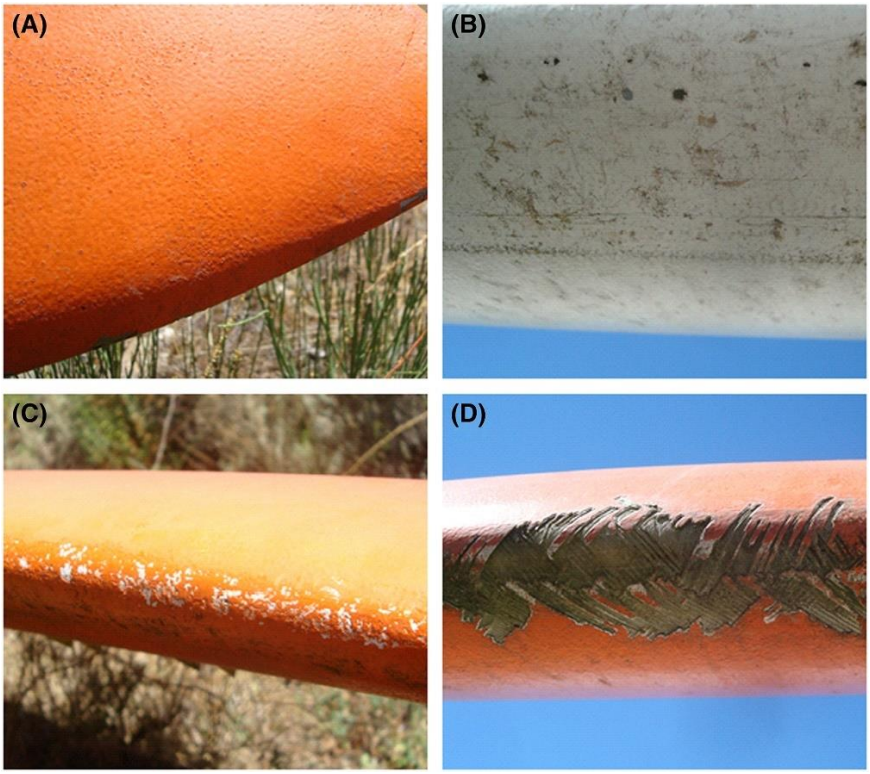

Figure 3. Progressive stages of rain erosion on the leading edge of wind turbine blades: A- pitting, B- cracking, C- cratering and D- delamination *[6]*.

To ensure smooth operation with optimal performance of the wind turbine, preventive measures are adopted such as preventive maintenance, reduction in rotor speed during heavy precipitation, and application of coatings on the leading edge of the wind turbine. Each of these methods has its own advantages and shortcomings. Offshore wind turbines are at a disadvantage as conducting preventive maintenance is not only difficult but expensive as well, while the turbine would be shut down for the duration of maintenance. While reducing the rotational velocity of the turbine blades during heavy precipitation may prolong the life of the turbine and therefore, the energy production in the long run. Enabling the turbines to operate under any condition without the need for a safe mode will help achieve higher outputs and help the transition towards renewable energy.

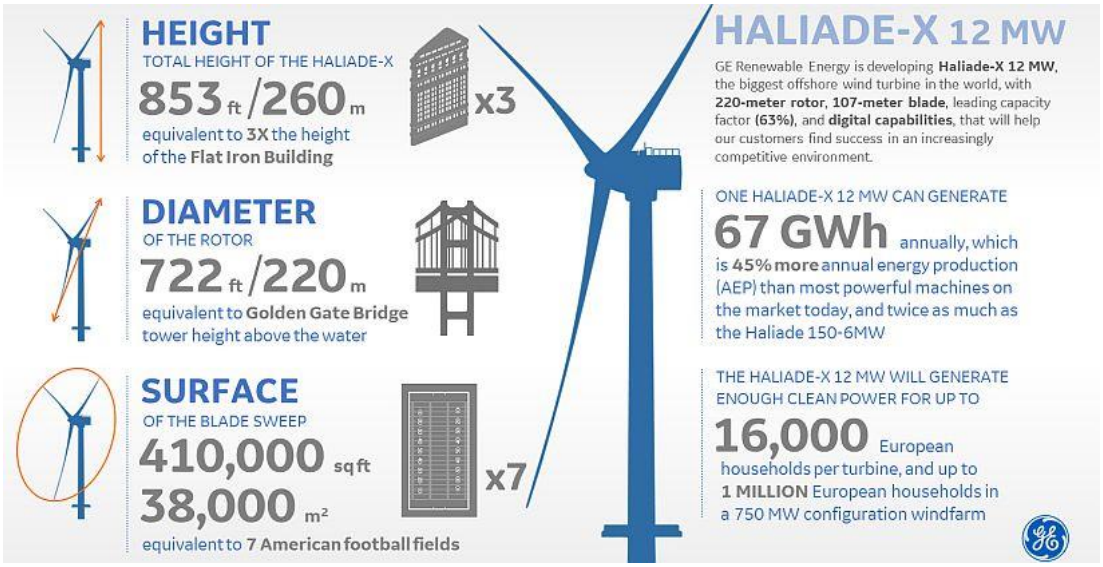

Figure 4. The GE-Haliade-X (Top) *[7]*.

The trend of increasing turbine dimensions to maximize outputs is continuing with the GE Haliade-X which is the largest turbine at the moment as shown in Figure 4. It has a rotor diameter of 220m and blade tip speeds exceeding 100 m/s, against which traditional coating system fail. Therefore, research in the field of coatings is ongoing to develop a new coating solution that can be co-bonded to the thermoset substrate like the Integrated Leading-Edge Protection (InLEP) project, an initiative by LM Wind Power. The types of coatings studied are thermoplastics such as acrylonitrile butadiene styrene (ABS), Thermoplastic polyurethane (TPU) and Polycarbonates, which are co-bonded to the substrate during the manufacturing process, shown in Figure 6. To sustain existing wind turbines' operability, thermosetting gelcoats are used to protect the eroded region of the wind turbine. The gelcoats and flexible coatings can be sprayed or applied via rollers onto the target surface [8]. Gelcoats are brittle and possess high acoustic impedance, while flexible coatings are ductile and possess lower impedance which dampens the induced stress waves by dissipating the energy from the impact [9]. However, these solutions are not ideal as they fail to protect the turbines at higher speeds. Hence, a new optimized solution is required that can be adapted across the industry to prevent erosion of wind turbine blades. This thesis is a part of the Integrated Leading-Edge Protection (InLEP) project, a collaboration between LM Wind Power and the University of Twente, whose goal is to develop an optimized thermoplastic Leading Edge Protection (LEP) system which can be integrated in the blade during its production process. Having an integrated LEP improves the aerodynamic efficiency and performance of the wind turbine as shown in Figure 5, and additionally, since the coating can be co-bonded to the substrate during the production process, it reduces the overall manufacturing lead time.

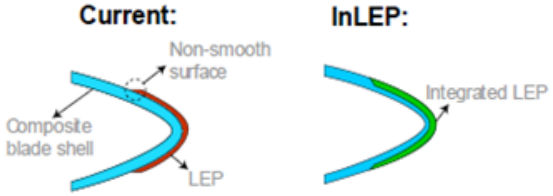

Figure 5. The co-bonded Integrated Leading Edge Protection (InLEP) coating system.

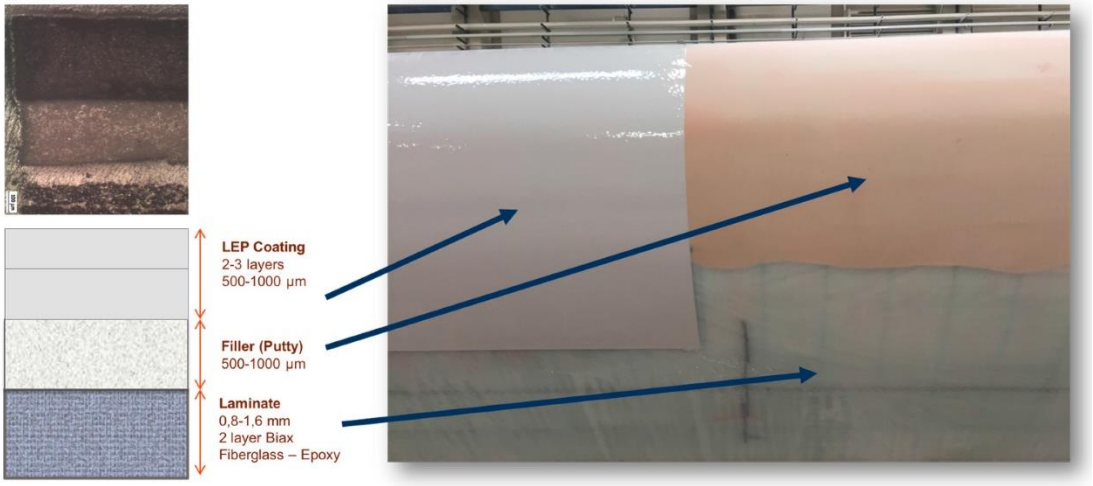

Figure 6. Coatings used as Leading-Edge Protection (LEP) in wind turbine blades *[10]*.

1.2 Droplet Impact Mechanisms

In this section the droplet kinematics are studied to understand wave propagation in the LEP and substrate, to develop an optimized LEP solution. Upon droplet impact, two distinct phases are observed in the droplet, namely, the compressible phase and lateral jetting phase. Whereas, in the substrate, three distinct waves are produced upon impact that propagate through the substrate – Surface or Rayleigh waves, Longitudinal waves, and shear waves. Understanding this interaction between the liquid and solid domain is crucial to study the erosion mechanisms occurring within the substrate.

- **Initial Compressible Phase**

  The moment when the droplet impacts the substrate, the contact edge between the two begins to spread out in a circular manner from the midpoint of impact creating a wavefront of compressed liquid in the droplet as shown in Figure 7a, travelling upwards through the droplet as there is no free surface through which the pressure can be released. The contact velocity, Vc is greater than the velocity of the shockwave, Cl. The compressed region of the droplet exerts a pressure on the substrate which is often assumed to be equal to the water hammer pressure. This is generally used to predict the impact pressure exerted on the substrate only in the initial phases, since it does not define conditions in the lateral jetting phase [11]. The water hammer pressure is defined as shown in equation (1):

$$P_{WH} = \rho_l C_l V \tag{1}$$

  P_{WH} – Water hammer pressure; ρ_l – Density of liquid; C_l – Velocity of shockwave; V – Impact velocity

- **Lateral jetting Phase**

  Lateral jetting occurs when the shock envelope overtakes the contact edge between the droplet and substrate, creating a free surface which enables the release of the compressed region via lateral jetting along the surface of the substrate as shown in Figure 7b. The lateral jets could possess velocities exceeding forty times the impact velocity. This high velocity

results in a high pressure along the wavefront which can exceed the water hammer pressure by a factor of 3 [9].

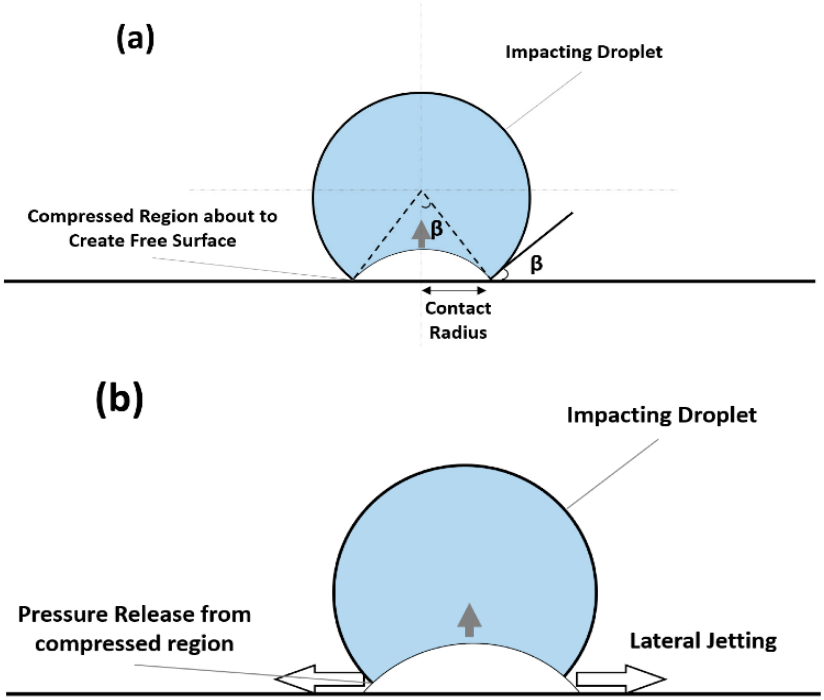

Figure 7. (a) Shockwave induced in the droplet during the initial compressible phase; (b) Lateral jetting and its initiation at the fluid-structure interface.

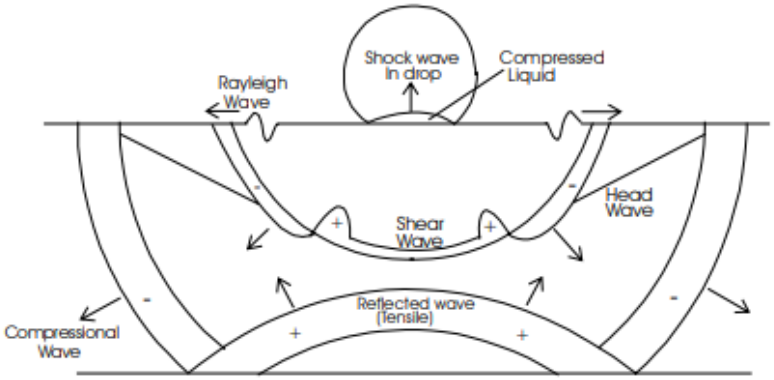

Figure 8. Stress waves induced in the substrate upon droplet impact.

The stress waves induced in the substate during droplet impact are shown in Figure 8 and are discussed subsequently.

- **Compressional Wave:**

  The compressional wave propagates through the material away from the point of impact. Based on material properties of the LEP and substrate, damage may be initiated by the compressional wave or the reflected, tensile wave propagating back towards the point of impact. At this stage, the tensile wave causes fracture damage within the material [8]. When the tensile wave interferes with the surface waves, it can amplify the surface waves while causing surface damage and fracture within the material. This is especially seen in thinner specimens.

- **Shear Wave:**

  As the contact area between the droplet and substrate increases, shear waves are created that propagate through the material. The propagation of these waves is determined by the acoustic properties of the LEP and substrate [9].

- **Rayleigh or Surface Waves:**

  The surface waves as the name suggests, propagate along the surface of the material. Surface waves can damage material by interacting with surface irregularities, this damage is amplified when the surface waves interact with the reflected compressional waves, also known as tensile waves, since they are tensile in nature.

The interaction and propagation of these waves is typically dependent on the material, impact, and geometrical parameters of the setup. A material with a higher impedance will absorb more of the wave energy as opposed to a material of lower impedance which would reflect more of the wave energy [10]. Similarly, a hard material will reflect a greater portion of the impact energy back into the droplet, thus, causing more lateral jetting. Conversely, a softer material will absorb more of the impact energy while deforming and reflecting less energy back into the droplet [8].

1.3 Erosion Mechanisms

When simulating droplet impacts, a single droplet is studied impacting the substrate. This does not depict erosion but rather helps predict the propagation of stress and location of damage initiation. The progression of erosion of the substrate can be divided into five distinct stages as shown in Figure 9. As can be seen, erosion occurs over a period of time or number of impacts and is therefore a fatigue mechanism. During the incubation stage the droplet impinges on to the substrate creating surface roughness and few pits [12]. This followed by the next stage where the pit formation is accelerated. At this stage, cratering begins when adjacent pits merge to form a crater. The next stage is when cratering is accelerated and results in severe erosion and mass loss. Due to the mass loss, the surface of the blade becomes rough with irregularities resulting in slower erosion rates. The last stage is the terminal steady erosion rate where the material fails and needs to be replaced.

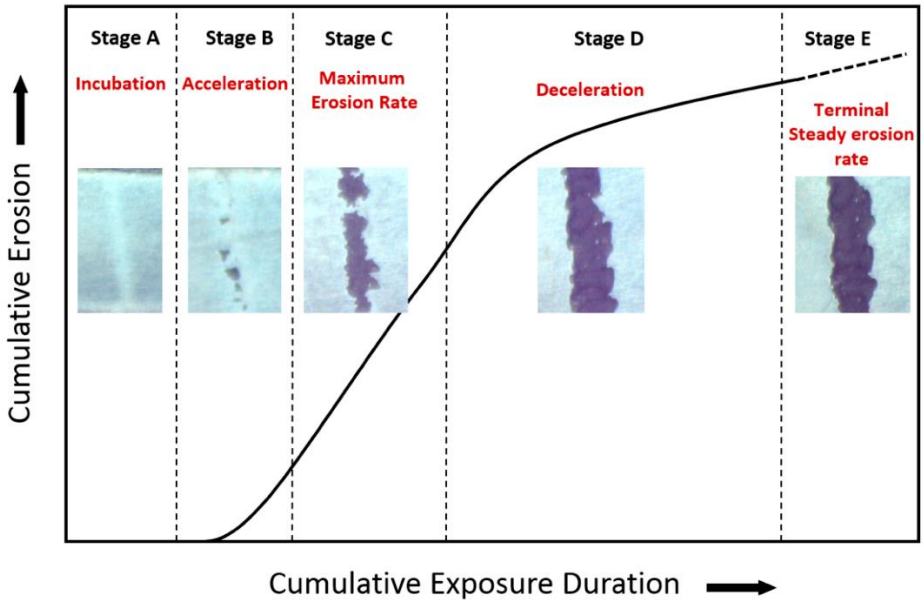

Figure 9. Cumulative mass loss due to erosion *[12]*.

The erosion mechanisms have been identified using experimental methods such as Rain Erosion Testing (RET). Testing is done to determine the life and failure modes of coatings used in the wind turbine blades. This is important since multiple high speed droplet impacts helps to determine the impact properties of the coating materials used. A typical RET setup has either a rotating or stationary specimen that is impacted by water droplets. The two setups employed to conduct RET are as follows:

- **Whirling Arm Setup**

  In this setup an artificial rain droplet field is generated through which the test specimen is spun by being affixed to a rotating arm. This results in a gradient of damage along the specimen.

- **Pulsating Jet Erosion Test Setup (PJET)**

  In this setup, the specimen remains stationary while water jet segments impact the specimen. This is achieved by a slotted rotating disc which slices the jet into segments with a constant jet length that impact the specimen [13]. The PJET setup is used at the University of Twente to study the damage mechanisms and plot the volume loss curve, which validates the damage location and stress concentrations predicted in the simulations.

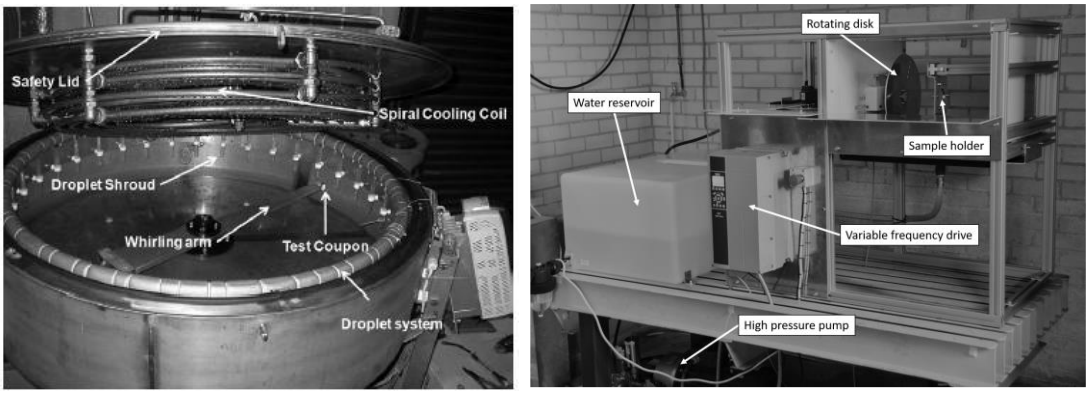

Figure 10. Whirling Arm Setup at the university of Limerick (Left) *[14]* and Pulsating Jet Erosion Test (PJET) setup at the University of Twente (Right) *[10]*.

1.4 Research Questions

The main objective of this thesis is to investigate the effect of different multilayer LEP materials on the stress field caused by droplet impact and to identify a viable LEP solution. Research has been done in the field of damage propagation in substrates using pulsating jet erosion setups and confocal microscopy. While damage mechanisms for certain materials, along with their lifecycles have been predicted using numerical modelling and experimentation. A viable co-bonded multilayered system has not been developed yet. Therefore, to study the effect of the induced stress waves in a multilayered substrate, the following research questions have been addressed:

1. How do the waves propagate in a multilayered substrate for different LEP materials?
    - How do waves propagate in polymeric materials?
    - How does the interaction of the stress waves affect the stress field?
    - How do material properties affect the stress field?

2. How does LEP thickness influence the stress field for different LEP materials?
    - What is the influence of a discrete interface on the stress field?

3. How does the interaction between a finite thickness interphase and the wavefront influence the stress field?
    - How does the stress field vary with a continuous interphase between the LEP and substrate?
    - How do the LEP and interphase thicknesses influence the stress field?

4. What mechanisms/parameters are important for LEP performance?
    - What types of stresses are observed in the system?
    - How do the stress concentrations influence the system?

These research questions are tried to be answered by using numerical modelling techniques in Abaqus for the materials studied. The upcoming chapters discuss the model set up and parameters, followed by preliminary results on polymeric materials. The chapters thereafter discuss the interphase regions in a multilayered system and its effect on the stress field. From these discussions, a set of design guidelines will be derived for a multilayered LEP-substrate system.

Chapter 2 : Methodology

2.1 Numerical Modelling

To replicate and study the kinematics of droplet impact in Abaqus accurately, a desirable numerical simulation with a low computational time is desired. Initially the impact simulations are done for pure polymers where the stress field in the LEP is studied. Subsequently a discrete interface, and a co-bonded LEP-substrate interphase were modelled and studied to answer the proposed research questions. In each of these simulations, a standard model is used, which will be discussed in this chapter. The standard model is developed by using a set of parameters which result in a consistent and comparable stress field for an optimized simulation time. To numerically simulate high speed – short duration droplet impacts, the following methods are commonly used:

- **Finite Element Modelling:**

  Here the mesh is applied to model geometry (standard lagrangian meshing methods) When simulating large deformations, the mesh tends to over deform leading to cell degeneration and reduction in model accuracy at the cost of computational power. Thus, this method is better suited for impact simulations with less to moderate deformation whilst it can be used to define a fluid domain, it is limited to internal volumetric meshes. (Commonly used in CFD analysis)

- **Eulerian and Eulerian/Lagrangian methods:**

  In this method the projectile (droplet) is modelled using an eulerian approach wherein the mesh is applied volumetrically to the model, while the target body (LEP) is modelled using standard lagrangian meshing methods. Therefore, when the body interacts with the eulerian domain, the resultant stress field provides good replication of the physical phenomena.

- **Smoothed Particle Hydrodynamics:**

  This is a mesh less method where the material is defined as particles with mass which interact with adjacent particles through the kernel function. This captures the high-speed large deformations in the fluid domain perfectly when combined with a lagrangian substrate. Therefore, a combination of SPH and lagrangian methods are used in this assignment since it is computationally less demanding.

Using the SPH method, an explicit analysis is carried out to simulate the droplet impact and the corresponding stress field in the material. To achieve accurate results the following assumptions are made:

- The rain droplet is considered spherical in shape.
- Impact occurs on a flat elastic solid.
- The target body is assumed free of imperfection with no initial surface roughness and pre-existing cracks.
- The droplet impact is assumed normal to the surface.

Parameters:

With the aforementioned assumptions, crucial parameter settings used to setup the model are shown in Table 1. While setting up the model in Abaqus, the droplet is modeled using the 'revolution' command and the substrate is defined using the 'extrusion' command in the *part menu.* Once the two parts are modeled, the parameters are setup as follows.

Table 1. Materials and properties used in SPH simulations.

Properties	**Density (kg/m^3)**	**E (Gpa)**	**υ**	**C_p (m/s)**	**μ (Pas)**	**V (m/s)**	**Diameter (mm)**	**Height (LxW) (mm)**
ABS (LEP)	1050	2.45	0.408	-	-	-	-	0.5(5x5)
TPU D60 (LEP)	1100	0.25	0.45	-	-	-	-	0.5(5x5)
TPU A80 (LEP)	1090	0.033	0.489	-	-	-	-	0.5(5x5)
Water (Droplet)	1000	-	-	1481	8.9e-4	100	2	-
Epoxy (Substrate)	1152	2.41	0.39	-	-	-	-	0.5–1.5 (5x5)

- **Material definition and assembly**

In Abaqus, the fluid domain is defined by the equation of state and the interactions of particles in the fluid domain are governed by the SPH method. Therefore, while defining the properties of water (fluid domain), in addition to the density (ρ), the acoustic velocity (C_p) and kinematic viscosity (μ) also need to be defined. For the substrate, the elastic properties like the Young's Modulus (E) along with the density and Poisson's ratio (υ) need to be defined.

In the assembly menu, the two parts are selected and assembled such that the droplet touches the surface of the substate and is aligned with the center of the substate as shown in Figure 15.

- **Meshing**

The droplet has a tetrahedral mesh while the substrate/LEP has a hexahedral mesh. The droplet has 80 elements seeded towards the bottom of the droplet. While the substrate has a region of interest at the center where the droplet impacts, thus has a denser mesh at the center through its thickness. The elements are defined to have a smooth transition from the center outwards, which was later optimized to achieve a smoother resultant stress field.

For the droplet, since the mesh is converted into particles, the PPD (Particle density) is set to 1. The kernel function, which governs the particle interactions, is set to cubic which provides a smooth simulation result. Once the mesh is defined, the set of nodes from the droplet is created called, 'DRPNDS'.

- **Step, interaction, and load definition**

Once the meshing is complete, a ‘dynamic, explicit’ step is defined from the step menu. The time period for this step is initially defined as 2 microseconds. The ‘variable field outputs’ defines the selected output variables at the selected times. Since an output at every 10 nanoseconds is required, a timepoint is defined for 0 to 2 microseconds with an increment of 10 nanoseconds.

From the interaction menu a new ‘General contact (explicit)’ interaction is selected with an interaction property of Normal and Tangential behavior.

The bottom surface of the substrate is encastred and the predefined field of velocity applied to the node set, ‘DRPNDS’. The velocity is applied in the Y direction with a magnitude of -100 (m/s).

- **Job submission**

The model is complete once the above parameters have been defined. The job is prepared and run with parallelization set to 8 threads for the following computer specifications:

Processor: Intel® Core ™ i7-9750H CPU @ 2.60GHz

Ram: 16GB

Operating System: Windows 10 Home, 64-bit

2.2 Standard Model

Before the standard model is developed, a few parameters need to be discussed in detail to address and understand their effects on the resultant stress field. These will help develop and optimize the standard model. The most crucial parameters are associated to the mesh, which defines the resolution of the stress field [15].

- **Kernel Function**

The kernel function governs the interaction of a particle with adjacent particles. The particles are independent and do not necessarily exhibit properties of a particle in general such as bonding. Rather they are based on discretized continuum partial differential equations. In Abaqus, there are 3 kernel functions, Cubic, Quadratic and Quintic. Cubic is the default kernel function yields the best interpolated result, being rounded, smooth and continuous while the Quadratic and quintic kernel functions yield relatively spikey results as shown in Figure 11. In this thesis, to obtain a smooth contact pressure gradient, the cubic kernel function is adopted.

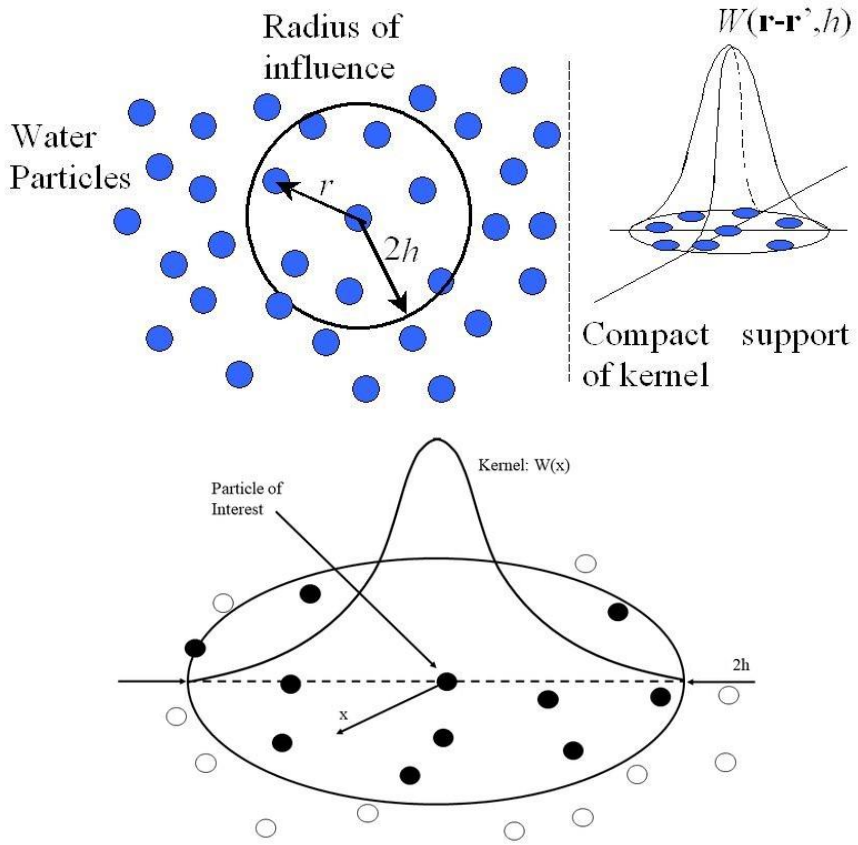

Figure 11. Quadratic kernel functions (Top) *[16]* and Cubic kernel functions (Bottom) *[17]*.

- **PPD**

  The particle density or number of particles generated per iso-parametric direction refers to the conversion of elements to particles. A PPD value of 1 signifies that each element in the SPH mesh will be converted to a particle. This directly affects the resolution of the resultant stress filed. While having more particles interact with the substrate yields better results, consequently the computational time increases along with localizations in the stress field as shown in Figure 12. Therefore, optimizing the mesh and setting the PPD to 1 would yield the best results, as opposed to only increasing the particles with a coarse mesh which would result in more increments and higher computational times.

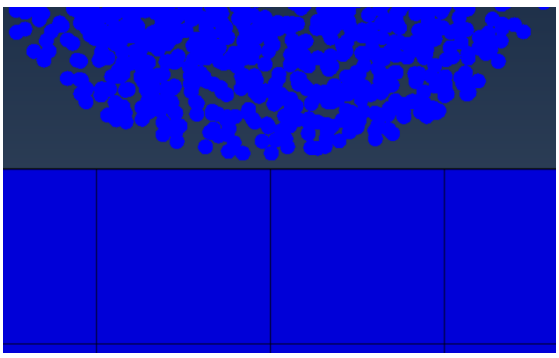

Figure 12. Ratio of particles to element sizes when PPD =1.

- **Mesh density**

The mesh density in a model can be controlled by optimizing the BIAS and seeding settings shown in Figure 13. BIAS refers to the concentration of the mesh elements defined from the center of a specific region. For a higher BIAS, the number of elements will be concentrated at the center and have a coarse transition to the adjacent elements, while for shorter BIAS, the elements are evenly concentrated, resulting in a smoother transition towards the adjacent elements. Seeding controls, the number of elements present in a specified region, thus directly affecting the mesh density in that region of the model.

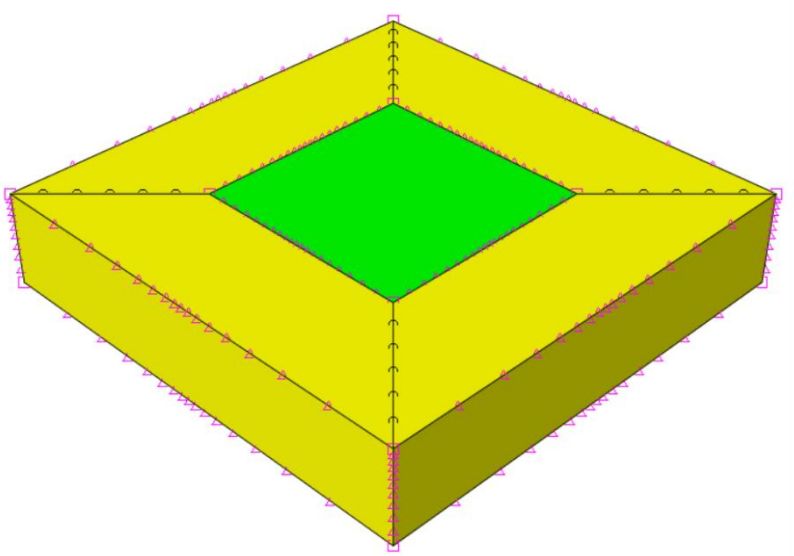

Figure 13. Seeding of mesh elements (center region) and BIAS control (periphery).

The goal of developing a standard model is to obtain a well-defined and comparable stress field with a relatively short computational time. The standard model serves to study and analyze the effects of droplet impacts on different LEP materials and thicknesses, and multisystem models. An initial model had a refined lagrangian mesh while the SPH mesh was relatively coarser, resulting in localization as shown in Figure 14. On the contrary when the SPH mesh was refined and the lagrangian mesh was relatively coarser, the computational time increased while the stress field in the substrate remained coarse due to the mesh. Several iterations were carried out to obtain a balanced mesh density between the two domains which is discussed in APPENDIX A.

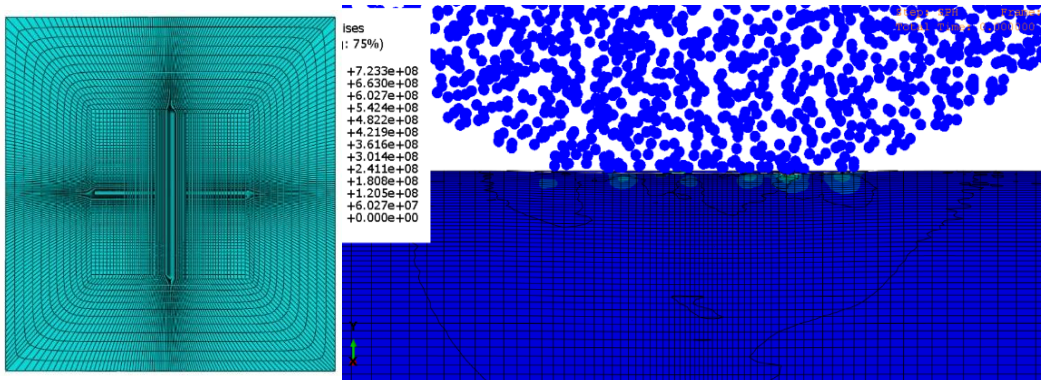

Figure 14. Localized stresses in substrate due to incorrect ratio of particles to elements. (Refined substrate, less particles interacting with more elements)

A turning point in developing the standard mesh was to optimize the dimensions of the substrate such that the adjacent region surrounding the central impact zone was discarded as it had no effect on the simulation. The dimensions of the substrate were optimized to 3mmx3mm with a varying thickness. Additionally, the center of the substrate had a higher mesh density, being the region of interest where the droplet would impact the substrate. Similarly, the SPH mesh was optimized by seeding the mesh towards the point of impact. Several iterations were performed to develop the standard model, the most promising iterations are discussed below.

- **SM#2**

  The SM#2 iteration shown in Figure 15 was meshed with 40 elements in the center with a double BIAS for a BIAS value of 2. However, at the periphery, the number of elements was set to 50 with a BIAS value of 5. Though this seemed to be a smooth mesh transition from the center to the periphery of the substrate, the resulting contact pressure transitioned via the BIAS, which was spikey and was therefore, not selected.

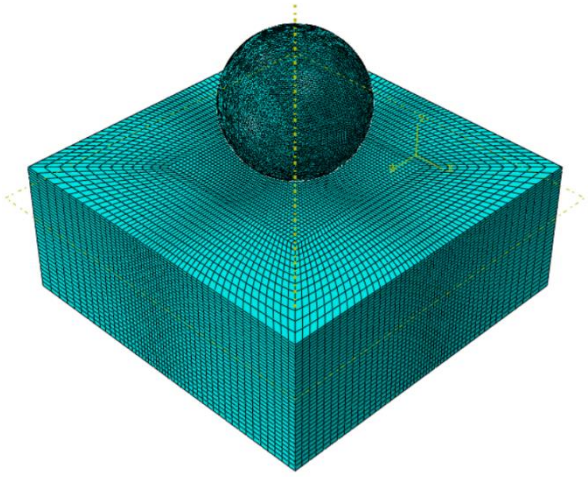

Figure 15. SM#2.

- **SM#3**

  This iteration provided the best results in terms of balancing the computational time and obtaining a smooth wavefront, as shown in Figure 16. Thus, it was selected to be optimized further. The central mesh had 60 elements with a double BIAS for a BIAS value of 2 with a smooth mesh transition towards the periphery.

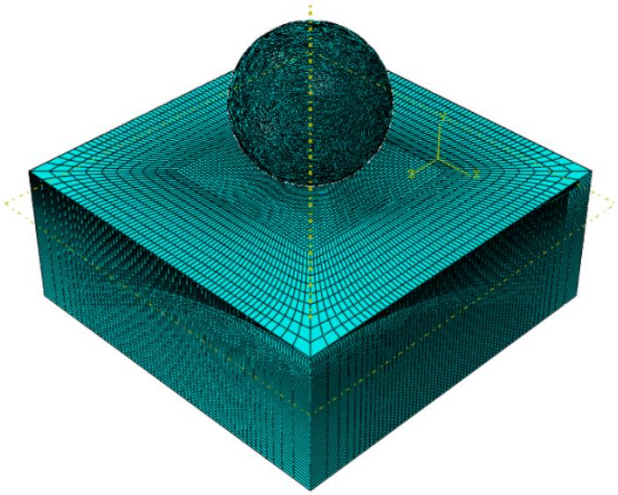

Figure 16. SM#3.

- **SM#4**

  This iteration had a relatively simple mesh with concentrations at the center as shown in Figure 17, however, the contact pressure was spikey along the BIAS similar to SM#2 and was therefore not selected.

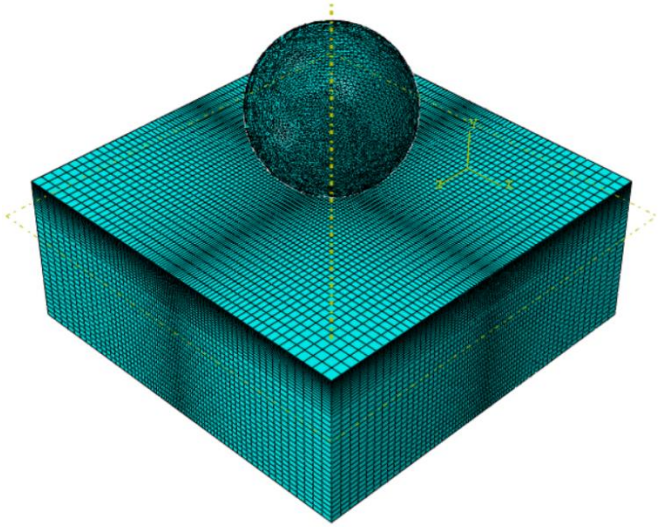

Figure 17. SM#4.

The blueprints of SM#2 and SM#3 were combined to further optimize the mesh and reduce the computational time. The central mesh of was optimized to 50 elements for a double BIAS with a BIAS value of 2, and 40 elements in the thickness coordinate with a BIAS value of 2 as well. Additionally, the droplet was segmented into two regions, initiating at 0.75mm from the bottom of the droplet. The smaller region had 150 elements defined, while the rest of the droplet was seeded for 40 elements with no BIAS. The resulting mesh is shown in Figure 18. These optimizations for a time period of 2 microseconds with outputs at 10 nanoseconds, yielded a good stress field with an approximate computational time of 7 minutes. This setup was used as the standard model for further simulations.

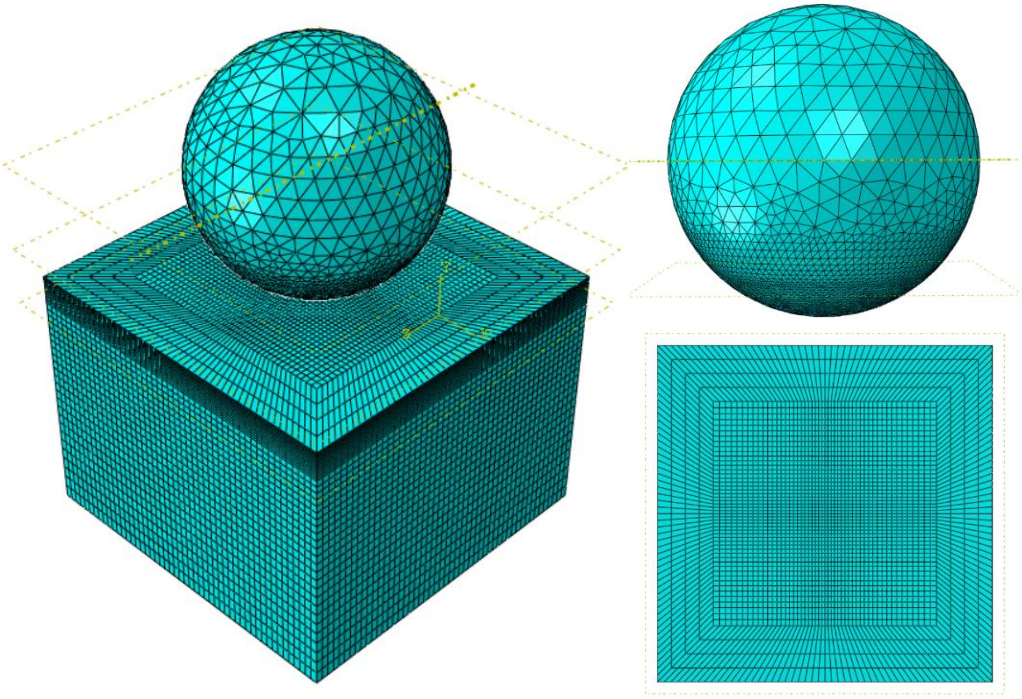

Figure 18. Optimized standard mesh.

2.2.1 LEP-Substrate Interface

LEP coatings protect the substrate from damage and are designed to function as a two-part subsystem. The material and thickness of the LEP affects the stress propagation in the LEP and substrate. To study these effects, the standard model is designed with a discrete interface in the thickness coordinate to distinguish the LEP and epoxy substrate as shown in Figure 19. Once the substrate is modeled, it is partitioned for a 2mm substrate with varying LEP thicknesses above the substrate. The dimension of the substrate is redesigned to 5mmx5mm since the stress spreads out wider into the substrate. This occurs at a later instance, therefore, to study the stress field in detail, the time period of the simulation is extended to 4 microseconds. The load definitions and boundary conditions for both the substrate and droplet remain the same.

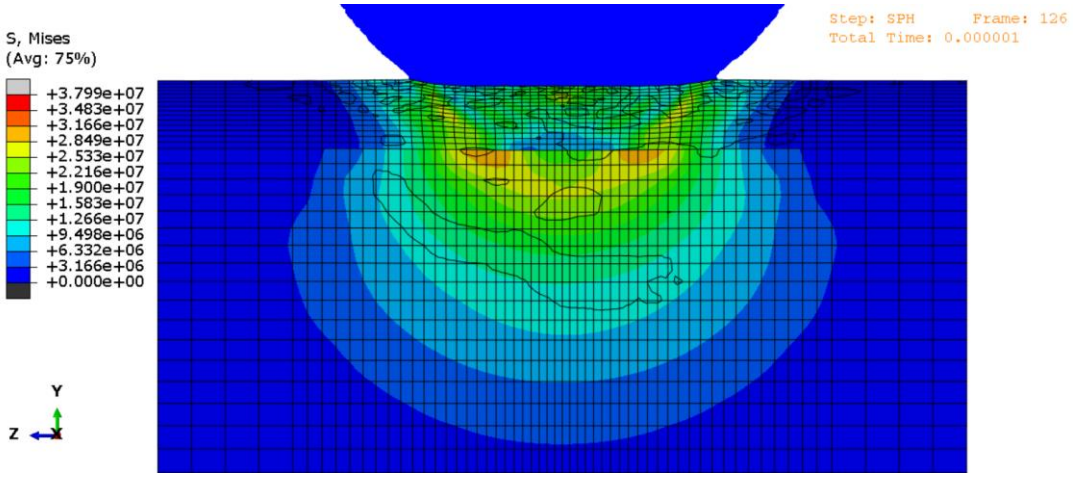

Figure 19. Stress field for a LEP-substrate system with a discrete interface (LEP - 0.25mm; TPU-D60).

The LEP thickness is designed for 0.25, 0.5, 0.75 and 1.0 mm with an epoxy substrate of 2mm. The influence of LEP thickness is discussed in Chapter 4. The number of elements in the LEP varies between 15 to 25 elements depending on the thickness of the LEP, while the LEP-substrate has a total of 40 elements in the thickness direction. For TPU D60, the droplet mesh was redefined to 130 elements in the smaller region along with the substrate mesh with central mesh region having 60 elements. Additionally, for TPU A80, the substrate mesh in the central region was reduced to 30 elements, with substrate dimensions of 5x5mm. These changes were adopted to reduce the numerical errors in the simulations.

2.2.2 Interphase System

In practice the LEP can be layered onto the substrate via the use of adhesives or co-bonding the LEP and substrate together. The prerogative of this thesis is to develop a suitable LEP solution for co-bonded LEP-substrate system. To achieve this, an interphase region between the LEP and substrate needed to be designed. The interphase has a linear transition between the material properties of the LEP and substrate. The interphase is modeled using functionally Graded Materials (FGM) in Abaqus which is discussed in detail in the following section. The primary change made to the model is the material definition, wherein a single material called the 'Gradient' is defined which varies across the thickness coordinate of the model. The discrete interface previously defined is no longer relevant and therefore the substrate has no sections. The influence of LEP and interphase thicknesses on the stress field is analyzed for TPU A80 and later implemented for other materials. Accordingly, the mesh had to be optimized to avoid numerical discontinuities in the substrate due the compliant nature of TPU A80. The changes made to the mesh in the model are as follows:

- The number of elements in the center reduced to 30, while the number of elements in the thickness direction was increased to 40 to obtain a better resolution of the stress field.
- The number of elements in the lower region of the droplet reduced to 130 elements, while the larger section retained the 40 elements previously defined.

The time period for the simulation remained constant at 4 microseconds along with the step, interaction, and predefined load (velocity) parameters. The above changes yielded a working model setup for the co-bonded LEP-substrate system.

2.3 Functionally Graded Materials (FGM)

To define the linear transition in material properties in the interphase region, the material properties need to be made dependent on the thickness coordinate. Since there is no direct method to achieve this in Abaqus, the temperature dependent data is used to define the correlation between material properties along the thickness of the model [18]. Unlike the LEP-substrate interface where the LEP and substrate materials had to be defined, in FGM, a single material is defined for the thickness of the material which includes the properties of both the LEP and epoxy, while enabling control over the interface thickness. In Chapter 5, the FGM is implemented to study the effect of interphase thickness on the stress field with a constant LEP thickness and vice versa.

For Abaqus to correctly interpret the temperature data as the thickness coordinate, a predefined temperature load needs to be defined in the load menu. Next, an analytical field needs to be defined which is done by selecting the function f(x). The expression field is selected,

and the datum is set to the local coordinate system along with the expression to define the point of origin for the thickness direction defined as follows: -Y-distance to surface of substrate.

This defines the analytical field, which is selected from distribution menu and the magnitude set to 1. Now the material properties have been defined for the thickness of the substrate, which is represented by the exponentially growing [+] signs along the substrate, signifying the direction thickness and its corresponding material properties from the top surface downwards as shown in Figure 20.

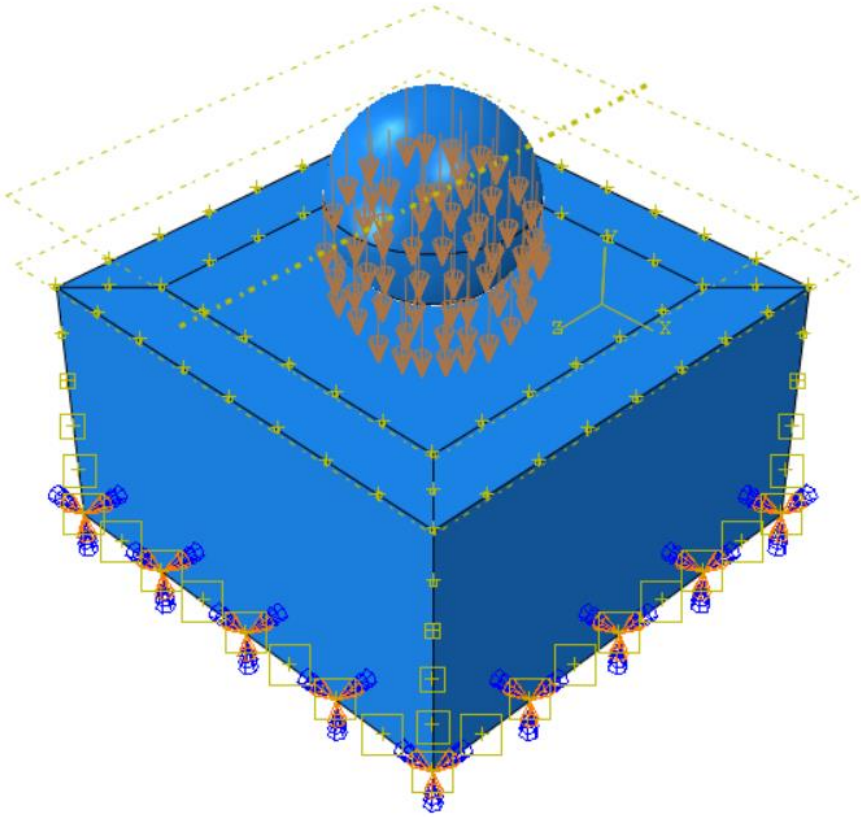

Figure 20. FGM and load definition in Abaqus.

Chapter 3 : Stress Response of Pure Polymers due to Droplet Impact

In this chapter the stress fields developed in pure polymeric materials are studied. An optimized model was used to study the characteristic response of the individual materials and their effects on the stress field. Here, the droplet diameter was 2mm and the LEP had dimensions of 3mmx3mm with a height of 2mm. The resultant stress field had good resolution with a low computational time.

3.1 TPU D60

Figure 21, shows the stress field observed for TPU D60. Upon droplet impact, a compressional wave is induced in the LEP which propagates radially outwards from the point of impact. The high energy density wave results in a stress concentration at the surface, which develops with time. The amplitude of these stresses varies from 10 to 12 MPa based on the instance of observation. Since the stress concentrations initially occur at the surface upon impact and propagate through the LEP to form a stress band region shown in yellow and red, suggests the stresses in the TPU D60 are superficial initially with internal stresses developing at a later period. This corresponds to a typical wave propagation induced in a material due to droplet impact.

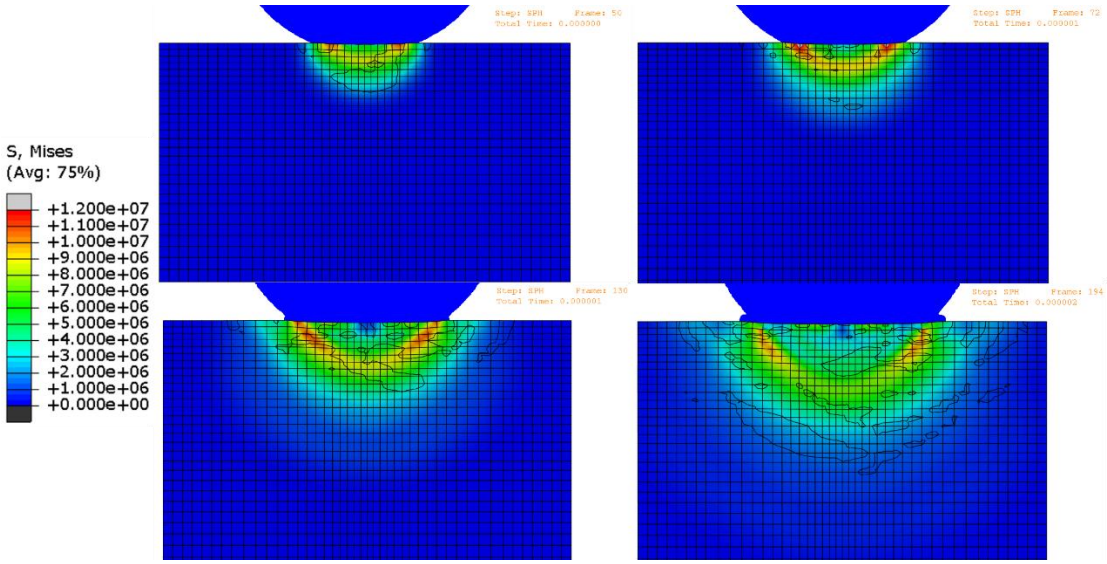

Figure 21. Von mises stress fields developing in a TPU D60 LEP.

3.2 TPU A80

Similarly, Figure 22 shows the stress field developed for TPU A80. The compressional wave induced in the LEP upon droplet impact propagates through the thickness of the LEP and results in a stress concentration at a later stage compared to TPU D60. The amplitude of these superficial stresses vary between 3 to 4 MPa. The amplitudes of stress observed for TPU A80 are lower than TPU D60, following the respective material characteristics. This suggests that for compliant materials like TPU A80, the stress concentrations are observed later on and have lower amplitudes of stress.

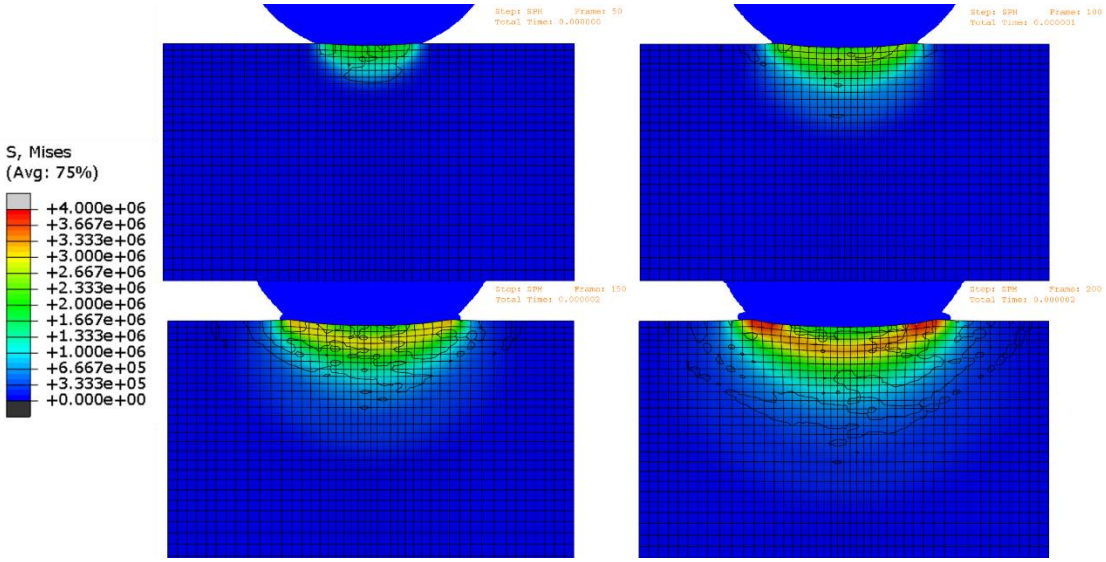

Figure 22. Von mises stress fields developing in a TPU A80 LEP.

3.3 ABS

Figure 23, shows the stress field developed for ABS. It is observed that the stress concentrations occur initially, and the observed amplitude of stress is the highest among the materials studied. The stress is concentrated at the surface as the high energy density compressional wave is induced in the LEP upon droplet impact. These stresses are superficial in nature and have an amplitude of 20 to 25 MPa, since ABS has a higher Young's modulus compared to TPU A80 and TPU D60. ABS, unlike TPU D60, dissipates the energy through the LEP and has typically negligible internal stresses compared to superficial stresses in this system.

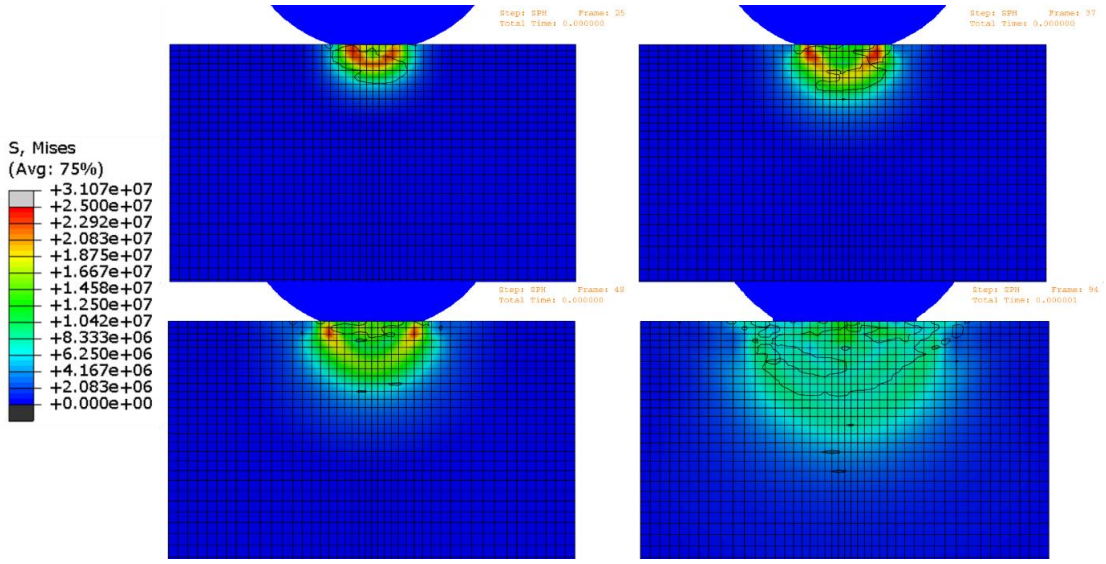

Figure 23. Von mises stress fields developing in an ABS LEP.

3.4 Summary

This chapter discussed the stress field developed in the studied LEP polymeric materials.

Table 2 shows the polymeric materials response to droplet impact and the corresponding type of stress along with the materials' Young's Modulus. The amplitude of stress observed varies for both, stiff and compliant materials. The instance at which the stress concentrations in the materials develop is different and is dependent on the material properties of the substrate. In TPU D60 and ABS, the stress is observed at the surface initially suggesting superficial stresses in the substrate. However, in TPU A80, these same stresses are observed at a later period of time. Therefore, it can be derived that for polymeric materials, superficial stresses are the dominant types of stress in the system. Furthermore, the contact pressure in the compliant materials is lower since the materials deform upon droplet impact, while in stiffer materials the contact pressure is greater since the material does not deform. This is observed by the higher amplitudes of stress in TPU D60 and ABS.

Table 2. Polymeric material properties and response to droplet impact.

Material	**Young's Modulus (GPa)**	**Instances of stress observed (Microseconds)**	**Amplitude of stresses observed (MPa)**	**Type of stress concentration**
TPU D60	0.25	50-194	12	Superficial
TPU A80	0.033	150-200	4	Superficial
ABS	2.45	25-48	25	Superficial

Chapter 4 : Discrete Interface Simulations

In this chapter, a multilayered system is analyzed to study the interactions between the LEP and epoxy substrate across a discrete interface, for different LEP materials and thicknesses. To study the influence of LEP thickness on the stress field, two distinct stress states are identified and compared for varying LEP thicknesses between 0.25mm and 1.0mm. The first stress state identified has initial stress concentrations in the system, while the second stress state is identified at a later period where the stress concentrations are located across the interface. This enables comparison between individual LEP materials and thicknesses, which helps identify an optimal LEP solution for each material.

The mechanisms of wave propagation are different in multilayered systems as compared to in pure polymers. In a multilayered system, upon droplet impact, compressional, shear and surface waves are induced in the system. However, when these waves reach the interface, a portion of these waves are reflected in the LEP, and the rest transmitted into the substrate. The interactions of these waves, especially the compressional wave and reflected compressional wave, also known as the reflected tensile wave, results in stress concentrations in the system. This increases the complexity of the observable stress states. In order to identify and study these mechanisms further, the following terminologies are important.

- **Impedance**

When an oncoming wave incurs a change in material properties, a portion of the wave is reflected into the LEP, and the rest transmitted into the substrate. The portions of the wave that are reflected and transmitted are governed by the impedance of the material which is calculated according to equation (2):

$$Z = \rho C \tag{2}$$

Where, Z is the impedance of the material, ρ is the density of the material and C the acoustic velocity of the material.

- **Acoustic velocity**

The speed at which the wave propagates through the LEP/substrate is equal to the acoustic velocity of the material itself. Therefore, if the calculated speed of the wave propagation is relatively close to the calculated acoustic velocity of the material, it indicates that the physical phenomena are accurately replicated in the simulation. The acoustic velocity is calculated as shown in equation (3):

$$C = \sqrt{\frac{E(1-\upsilon)}{\rho(1+\upsilon)(1-2\upsilon)}} \tag{3}$$

Where, C – acoustic (pressure wave) velocity, E - young's modulus, υ *- poissons ratio and ρ - density of the material.*

- **Transmissibility ratio**

The transmissibility ratio is obtained from the ratio of transmitted to incident stresses as shown in equation (4). A higher transmissibility ratio indicates that a higher portion of the waves are transmitted across the interface.

$$\frac{\sigma_{Tcs}}{\sigma_{Ics}} = \frac{2Z_s}{Z_c + Z_s} \tag{4}$$

The subfixes T and I in σ_{Tcs} and σ_{Ics} correspond to the transmitted and incident stresses, respectively at the coating-substrate interface.

4.1 Influence of LEP thickness on the stress field

In this section the second stress states are compared for the subsequent LEP's and LEP thicknesses since this stress state has a mature stress state where the stress concentrations are across the interface. This helps study the effect of LEP thickness on the stress field.

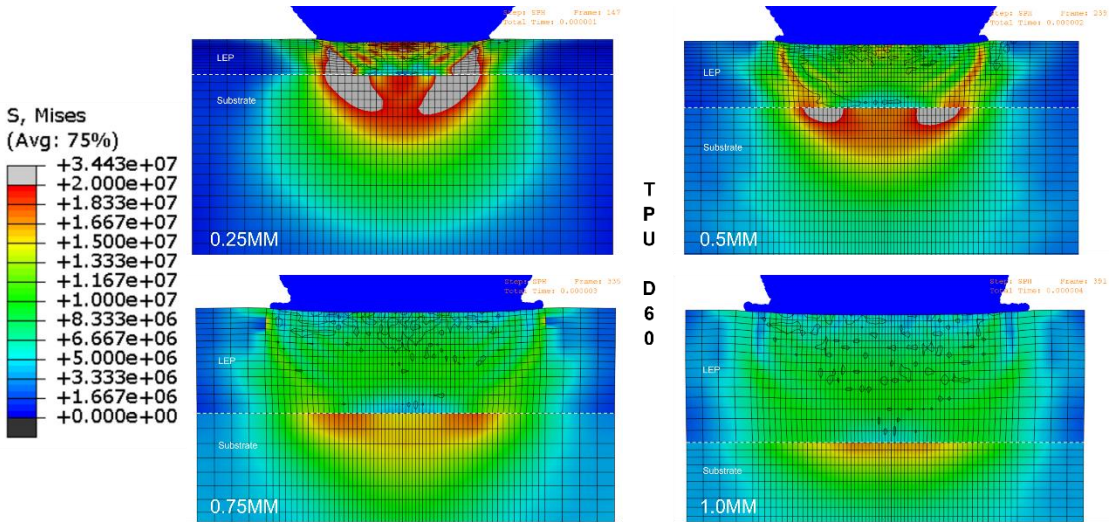

Figure 24. Von Mises stress field for varying LEP (TPU D60) thicknesses.

Calculating the acoustic velocity for TPU D60 from equation (3) yields 928.47 m/s, and equation (2) gives the impedance value for the LEP and substrate as 1021324 kg/m^{2}s and 2353319.74 kg/m^{2}s, respectively. The transmissibility ratio obtained from equation (4) results in a value of 1.39 which suggests a high transmissibility of stresses into the substrate from the LEP as seen in Figure 24.

In TPU D60, the 0.25mm LEP has the highest stress concentration, while the 1.0mm LEP has the lowest stress concentrations. In the 0.25mm LEP the stress is concentrated at the interface and in the LEP, along its surface and the center of the LEP. Due to the thinner thickness of the 0.25mm LEP compared to the others, the stress at the center and surface of the LEP merge, forming a region of stress concentration. As the LEP thickness increases, these concentrations remain distinct but faint due to the dispersion of energy over time with increasing thickness. As the LEP thickness increases, the stress concentration in the LEP dissipates, since the reflections in the system occur at a later period of time due to the increase in distance traversed by the waves. Therefore, thicker LEP's seem to be ideal for typical LEP coatings. However, an optimized solution should utilize the material properties of both the substrate and LEP effectively to dissipate the impact energy, such as the 0.5mm LEP for TPU D60.

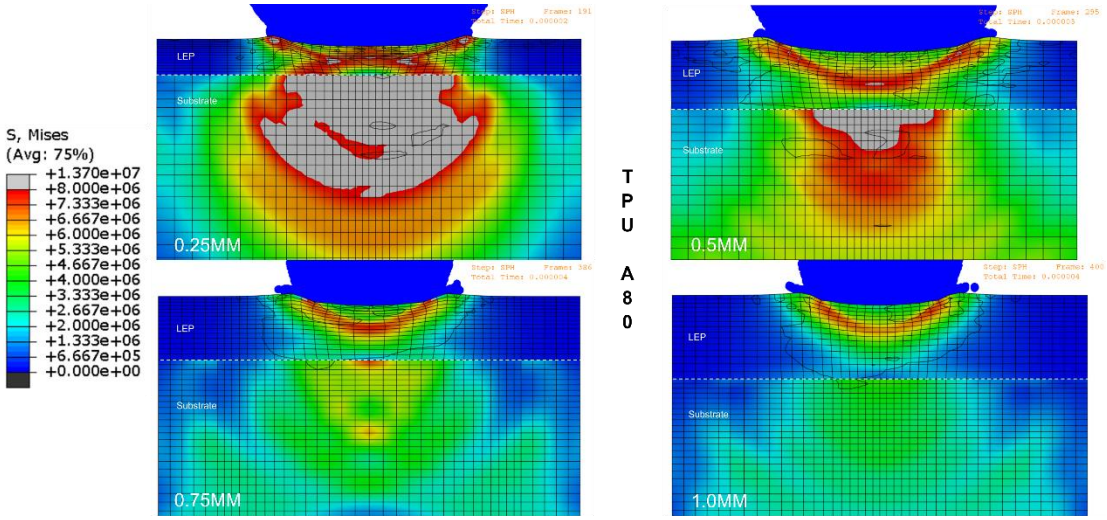

Figure 25. Von Mises stress field for varying LEP (TPU A80) thicknesses.

The calculated acoustic velocity of TPU A80 from equation (3) is 687.219 m/s, while the transmissibility ratio obtained from equation (4) results in a value of 1.53. This is higher compared to TPU D60, suggesting a higher transmission of stresses into the substrate from the LEP as shown in Figure 25.

In TPU A80, similar to TPU D60, the highest amplitude of stress is observed in the 0.25mm LEP, with the lowest amplitude observed in the 1.0mm LEP. As discussed previously, TPU A80 is a more compliant material, which results in lower amplitudes of stress in this system compared to TPU D60. In the 0.25mm LEP, being the thinnest LEP, the superficial stress at the surface of the LEP merges with the stress concentration at the center of the LEP caused due to the interaction between the compressional and reflected tensile waves. This results in the formation of a stress band (stresses greater than 6 MPa) in the LEP which is distinctly visible in thicker LEP's. Optimally utilizing the material properties of the LEP and substrate to support the other by energy dissipation, the 0.75mm LEP shows promising results. The internal stress in the system develops over time due to the reflections in the system occurring later on, while for thinner LEP's this is observed relatively sooner, but due to the inherent shorter thickness of the LEP, superficial stresses are dominant in these systems.

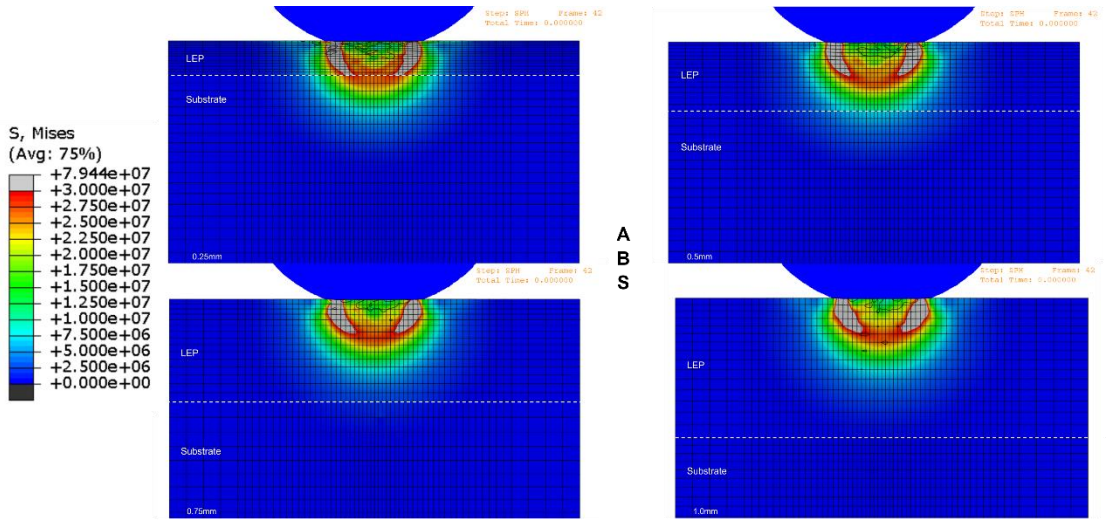

Figure 26. Von Mises stress field for varying LEP (ABS) thicknesses.

ABS is the stiffest LEP studied which shares its properties with epoxy, and has a transmissibility ratio of 1. Therefore, the reflections in the system are minimal and the superficial stresses are the dominant mechanism in this system, as shown in Figure 26. Therefore, a singular instance across varying LEP thicknesses is considered to study the influence of LEP thickness on the stress field. For LEP thicknesses of 0.25mm and 0.5mm, the wavefront permeates into the substrate, while for the 0.75mm and 1.0mm LEP's the wavefront is constricted to the LEP itself, due to the increased LEP thickness. The high superficial stress in the LEP is caused by the high energy density induced compressional waves resulting from the high contact pressure in this system. Since the substrate and LEP share material properties, an optimal LEP solution would yield even energy dissipation through the system, like the 0.25mm or 0.5mm LEP's.

4.2 Discussions

The three materials considered for this study are TPU D60, TPU A80 and ABS. Possessing different strength and elastic properties, they can provide valuable insights into the interaction between the LEP and substrate during droplet impact and the subsequent mechanisms involved in stress propagation through the system across a discrete interface.

Two distinct stress states were considered and analyzed for different materials, an initial state and a maturing/matured state where the stress field shows the critical interactions and corresponding effects between the stress waves in the system. The first stress states for TPU D60 and TPU A80, at key LEP thicknesses of 0.5mm and 0.75mm, are shown in Figure 27.

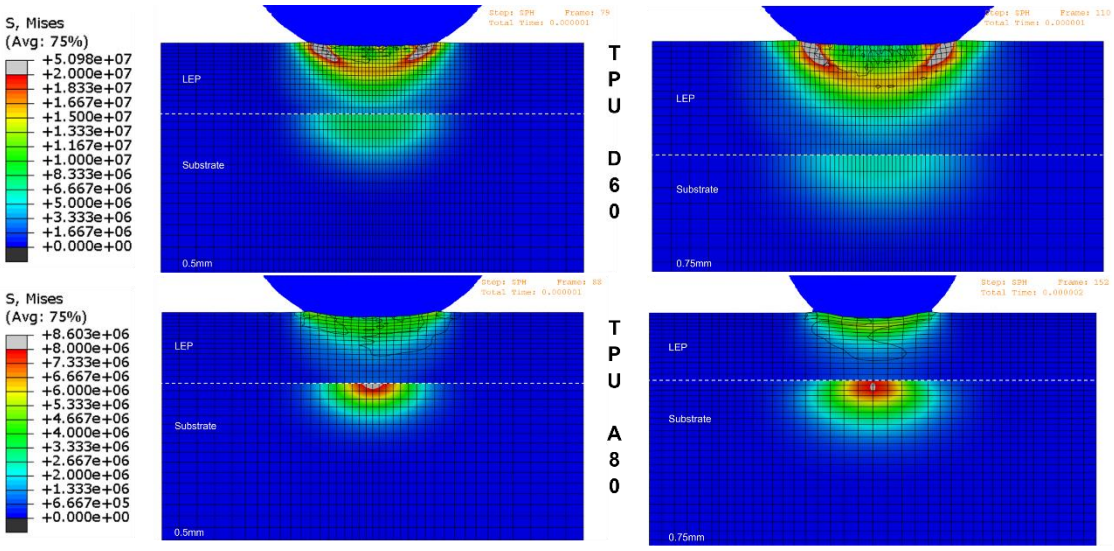

Figure 27. Comparison of the first stress states for LEP thicknesses of 0.5mm and 0.75mm in TPU D60 and TPU A80.

The stress states for both materials are unique, however, instances at which these stress states occur are different for the two LEP thicknesses. The amplitudes of stress can be compared for the two LEP's as shown in Table 3.

Table 3. Analysis of first stress states for TPU D60 and TPU A80.

LEP material	First stress state (microseconds)	LEP thickness (mm)	Stress amplitude (MPa)
TPU D60	0.79	0.5	50.98
	1.10	0.75	44.16
TPU A80	0.88	0.5	8.60
	1.52	0.75	8.13

A key observation from Table 3, is the variation in stress amplitudes for the two materials. TPU A80 has an 80% lower stress amplitude compared to TPU D60. This could be due to the higher contact pressure and stiffness of TPU D60 compared to TPU A80. Additionally, the more compliant TPU A80 relies on the substrate to disperse the impact energy as shown in Figure 27, while in the stiffer TPU D60 the stress is dispersed through the LEP with the substrate supporting the LEP. This is evident from the stress concentrations observed in both the materials. The stress concentrations develop in the LEP for TPU D60 whereas for TPU A80, the stress concentrations develop at the interface.

Observing the second stress state for TPU D60 and TPU A80 as shown in Figure 28, the time periods and the maturing stress fields are visible which highlight the effect of material parameters on wave propagation as the stress concentrations for the two LEP's are observed at different locations. Figure 28 provides an overview of the stress amplitudes and instances at which the second stress state is observed in the 0.5mm and 0.75mm TPU LEP's.

Table 4. Analysis of second stress states for TPU D60 and TPU A80.

LEP material	Second stress state (microseconds)	LEP thickness (mm)	Stress amplitude (MPa)
TPU D60	2.39	0.5	33.87
	3.35	0.75	20
TPU A80	2.95	0.5	9.93
	3.86	0.75	9.03

As discussed for the first stress state, the stress concentrations in the second stress also highlight a pattern in the stress field dependent on the material properties of the LEP. The second stress state shows a matured stress field where the waves have propagated and dispersed majority of the impact energy. Analyzing the stress field for TPU D60, this matured field suggests that, contrary to the first stress state, the stress is concentrated at the interface for both the 0.5mm and 0.75mm LEP's, respectively with trailing stress concentrations in the LEP. These are caused by the interaction of the oncoming compressional wave with the shear and reflected tensile waves in the system. Since this stress state is observed at a later period of time,

the energy density of the waves reduces over time with increasing LEP thickness. Table 4 highlights the lower amplitudes of stress for later periods of time and increasing LEP thickness respectively. Similarly, for TPU A80, converse to the first stress state, the primary stress concentration is observed at the center of the LEP, while the stress concentration at the interface reduces with increasing LEP thickness as can be seen. The stress concentrations in the LEP are typically due to the interaction of the compressional and tensile waves, while the stress concentrations at the interface are due to the interactions between the transmitted and shear waves respectively.

As can be observed for the two materials, the two stress states show different results for the selected LEP thicknesses. However, the mechanism of wave propagation between the two materials and stress states is identical, in the fact that they are governed by the reflections in the system. The intrinsic material properties of the two LEP's affect the way the energy is dissipated through the system, and thus, the subsequent reflections in the system. The stiffer TPU D60, initially absorbs the impact energy, then dissipates it through the system while the substrate supports the LEP, leading to higher stress concentrations at the interface. Conversely, the compliant TPU A80, initially cushions and transmits the impact energy into the substrate and later on dissipates the stress across the LEP-substrate system.

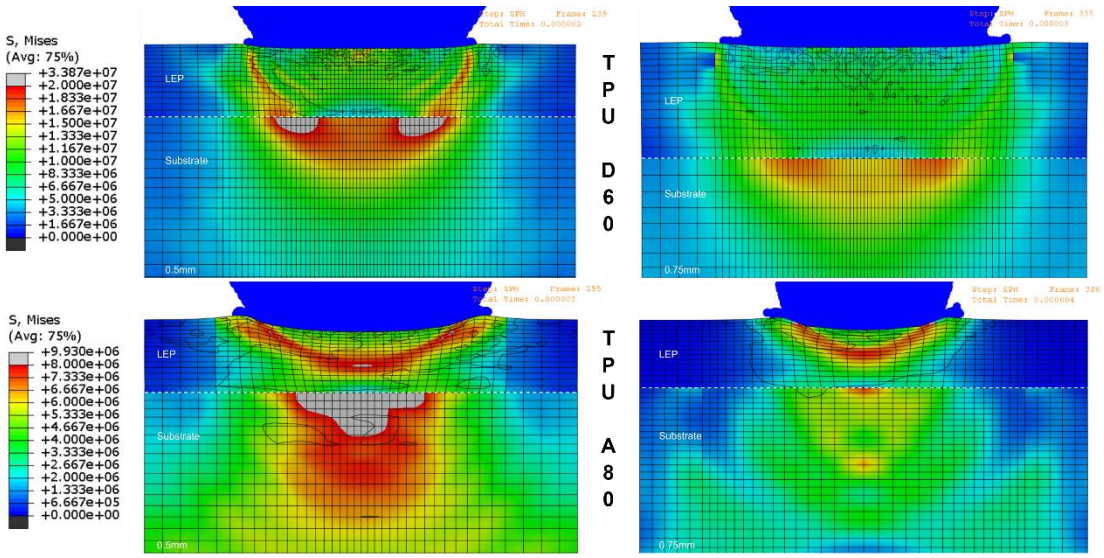

Figure 28. Comparison of the second stress states for LEP thicknesses of 0.5mm and 0.75mm in TPU D60 and TPU A80.

ABS and epoxy have almost identical material properties which results in a smooth and continuous, combined wavefront across the interface. Therefore, the energy is dissipated through the LEP and substrate equally, with superficial stress concentrations along the surface of the LEP. Unlike the TPU D60 and TPU A80 LEP's, the mechanism of wave propagation and stress concentration in the system is driven by the high energy density compressional wave induced in the LEP upon droplet impact. Since the material properties of the system are almost similar, the reflections in the system are minimal, resulting in minimal internal stresses and high superficial stresses as shown in Figure 29.

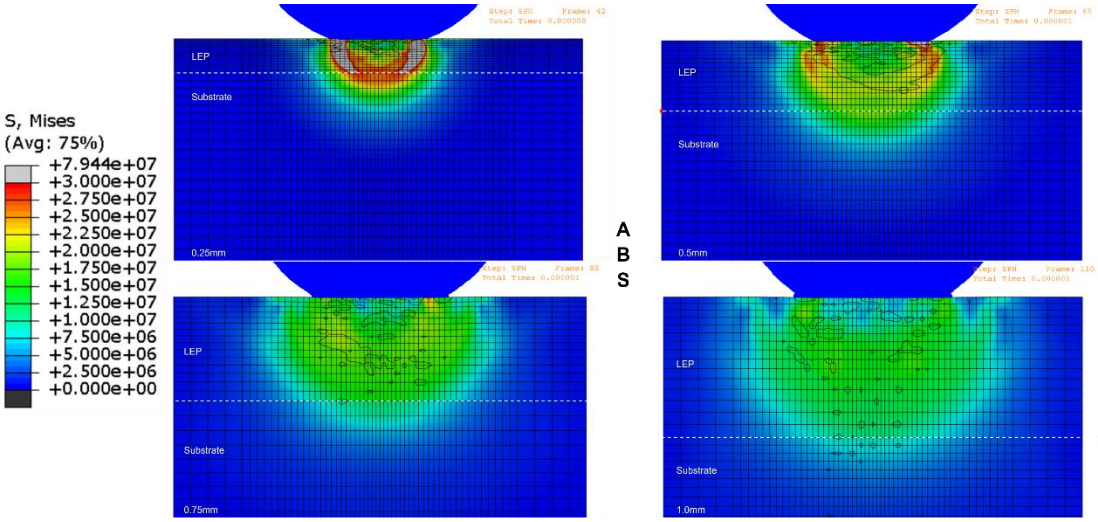

Figure 29. Similar stress states for varying LEP (ABS) thicknesses.

Chapter 5 : Interphase Simulations

In this chapter an interphase region is designed between the LEP and substrate that has a linear transition in the material properties across the thickness coordinate in the model. This linear transition is representative of a co-bonded LEP and substrate. As mentioned in Chapter 2, this interphase is defined using Functionally Graded Materials (FGM). In the following sections, the interphases are analyzed for TPU A80 with varying LEP and interphase thicknesses. Interphase thicknesses ranging from 0.1mm to 0.4mm are studied with corresponding LEP thicknesses of 0.3, 0.5 and 0.7mm respectively. The goal is to obtain a holistic understanding of the influence both LEP and interphase thickness on the resulting stress field. In order to achieve this, two stress states observed at 1.75 microseconds and 3.50 microseconds are studied.

.

5.1 LEP – 0.3mm (Interphase – 0.1, 0.3, 0.4 mm)

Figure 30 shows the first stress state observed across the interphases for a 0.3mm LEP. The stress is concentrated across the interphase region with a high amplitude of 10.5MPa, while the amplitude of stress in the adjacent LEP and substrate regions is lower. In the 0.1mm interphase, the stress is concentrated across the interphase region and continues in the substrate as well. This could be due to the rapid transition in material properties across the interphase region. As the interphase region increases, the same stress concentration in the substrate is not visible due to the larger and gradual interphase region.

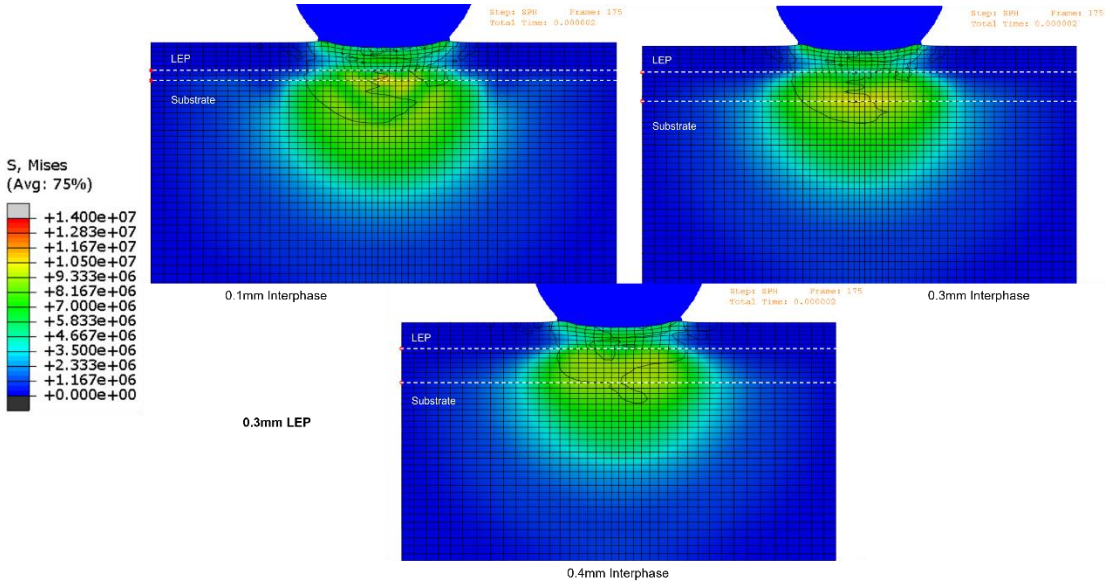

Figure 30. Von Mises stress fields for Interphases 0.1mm (Top Left), 0.3mm (Top Right) and 0.4mm (Bottom) with a 0.3mm LEP.

The second stress state observed is shown in Figure 31. Here, the influence of the interphase thickness on the LEP and substrate is more distinct. In the 0.1mm interphase, the stress is concentrated in the lower portion of the interphase region, which transitions into the substrate. The highest stress in the LEP is located at the surface near the point of impact and at the surrounding region across the LEP-interphase region. At this location, the central region has a comparatively lower amplitude of stress. This is due to the inertia of the waves caused by the change in material properties. Additionally, this rapid change in material properties, also

results in the stress concentration observed at the interphase region. The amplitude of stress observed is 14MPa which is higher than the stress observed in the first stress state at 10.5 MPa. This suggests that the stress observed at these stress states are the internal stresses of the system. In the 0.3mm and 0.4mm interphases, the stress is concentrated across the interphase regions with an amplitude of 10.5MPa. This is lower than the stress observed in the 0.1mm interphase, indicating the influence of interphase thickness on the system. When the interphase is thinner, the stress wave interacts earlier when compared to thicker interphases, although it should be noted that the interaction between the waves remains analogous for different interphase thicknesses, the interaction occurs at a later period proportional to the increasing thickness as shown in Figure 30 and Figure 31. Since the interphase region is a transition in properties between the two layers, the resultant impedance would cause interaction between the compressional and tensile waves. The low stress concentration region within the interphase region is distinct in the 0.3mm and 0.4mm interphases. Furthermore, the wavefront is noticeably smoother and gradual as the interphase thickness increases.

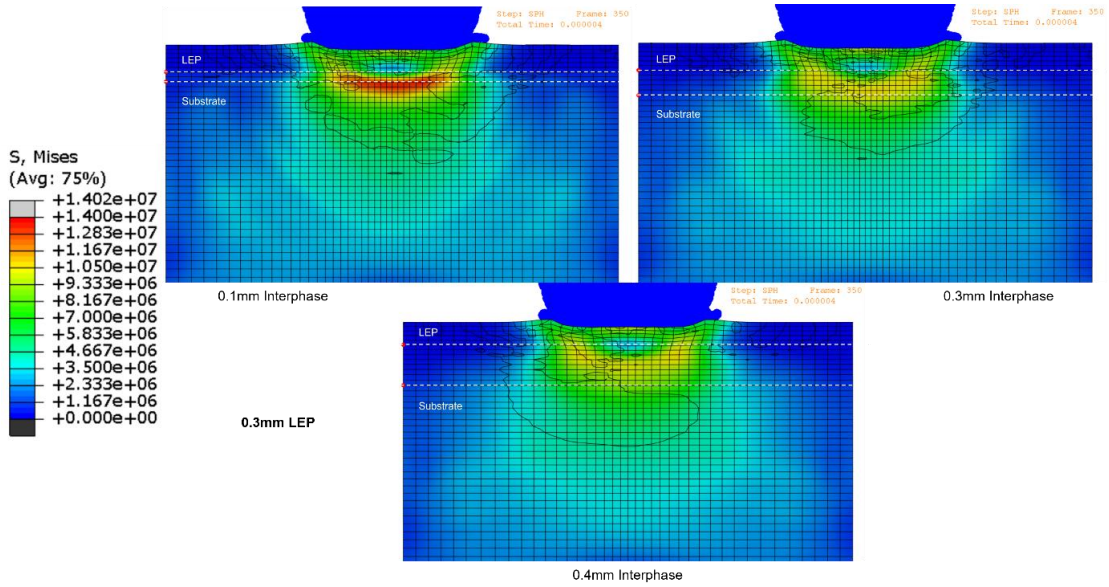

Figure 31. Maturing Von Mises stress fields for interphases 0.1mm (Top Left), 0.3mm (Top Right) and 0.4mm (Bottom) with a 0.3mm LEP.

5.2 LEP – 0.5mm (Interphase – 0.1, 0.3, 0.4 mm)

Figure 32 shows the stress field developing for different interphase thicknesses in a 0.5mm LEP. Similar to the 0.3mm LEP interphases, a smoother wavefront is observed as the interphase thickness increases. In the 0.1mm interphase, the stress is concentrated in the substrate below the interphase region, while in the interphase region a small central stress concentration is initiated. In the 0.3mm and 0.4mm interphases, the stress concentration gradually moves towards the interphase-substrate region. The stress is predominantly located in the interphase region in the 0.4mm interphase. This suggests that the waves traverse faster across shorter interphases due to the rapid change in material properties. When compared to the 0.3mm LEP interphases, the stress amplitudes are relatively lower and the stress across the interphase is minimal.

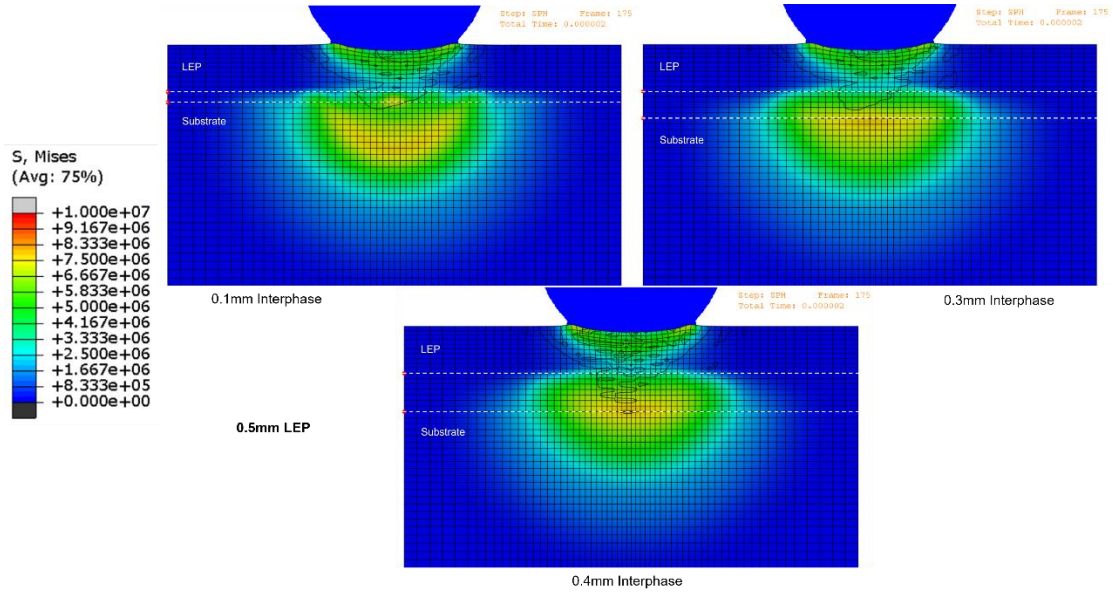

Figure 32. Von Mises stress field for interphases 0.1mm (Top Left), 0.3mm (Top Right) and 0.4mm (Bottom) with a 0.5mm LEP.

Observing the second stress state for the 0.5mm LEP interphases as shown in Figure 33, a distinct stress concentration region in the LEP is observed. This stress concentration forms a banded region resulting from interaction between the oncoming compressional and reflected tensile waves in system. Furthermore, in the 0.1mm interphase, the stress is concentrated in the interphase region with an amplitude of stress of 8.5 MPa, while in the 0.3mm and 0.4mm interphases, the amplitude of stress is around 7 MPa. Thicker interphase regions have lower stresses which could yield a suitable LEP solution, as the transition in material properties is gradual, while the stress is concentrated in the LEP shielding the substrate.

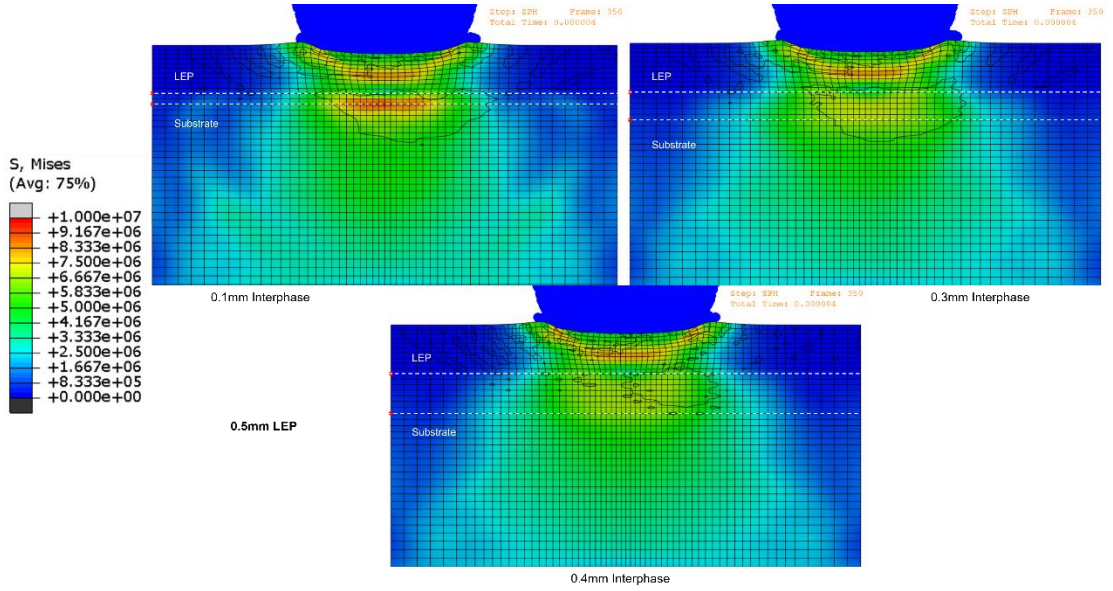

Figure 33. Maturing Von Mises stress field for interphases 0.1mm (Top Left), 0.3mm (Top Right) and 0.4mm (Bottom) with a 0.5mm LEP.

5.3 LEP – 0.7mm (Interphase – 0.1, 0.3, 0.4 mm)

Figure 34 shows the first stress state for the interphases in the 0.7mm LEP system, where the stress across the interphase is the lowest compared to the 0.3mm and 0.5mm LEP systems. This is because the waves transverse a larger distance before reaching the interphase region. Similar to the previous LEP systems, the 0.1mm interphase shows a (slight) flutter in the wavefront formed at the LEP-interphase region caused due to inertia of the traversing waves across the rapidly transitioning interphase region. At this instance the stress is lightly concentrated in the lower portion of the interphase region.

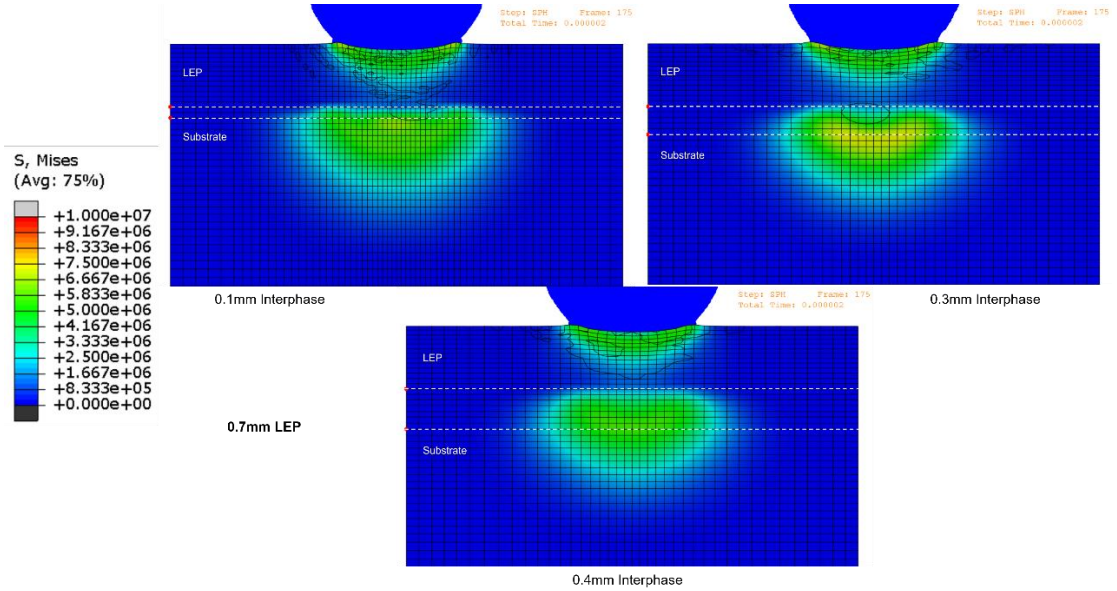

Figure 34. Von Mises stress field for Interphases 0.1mm (Top Left), 0.3mm (Top Right) and 0.4mm (Bottom) with a 0.7mm LEP.

The stress field observed in the second stress state is shown in Figure 35. Similar to the 0.5mm LEP system, a stress concentration band is observed in the LEP. The highest stress is observed at the surface with visible interactions between the compressional and tensile waves in the LEP. Across the interphase, the amplitude of stress is lower as the thickness of the interphase increases. The adjacent wavefronts become smoother and rounded as the interphase thickness increases. The amplitude of stress observed across the interphase is the lowest when compared to the 0.3mm and 0.5mm LEP thicknesses, since the stress spreads further before being reflected and transmitted causing the energy to be absorbed by the LEP initially and supported by the interphase and substrate at a later stage.

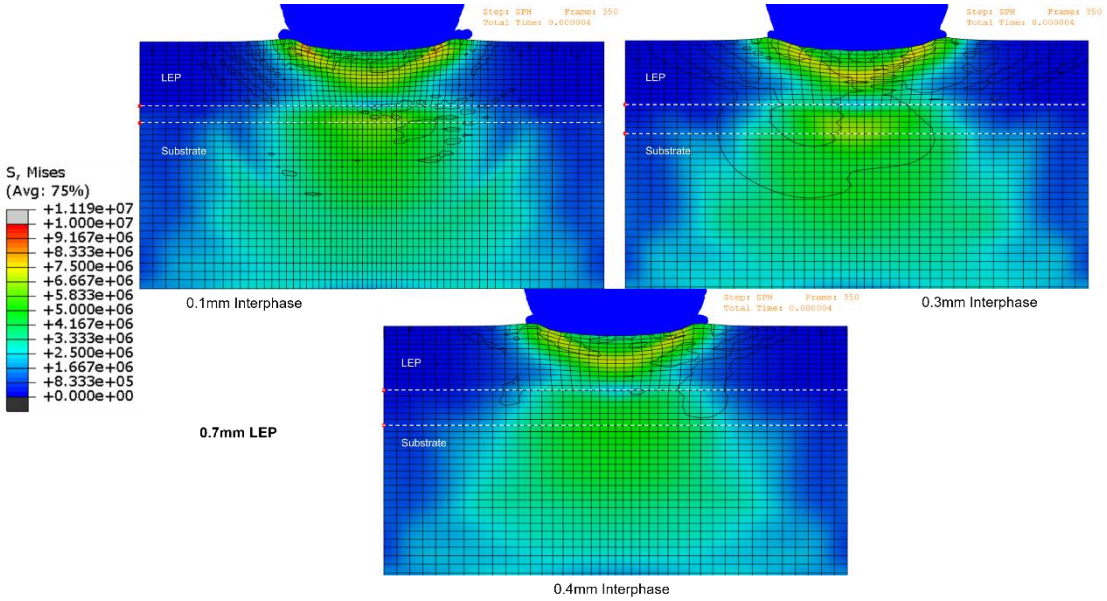

Figure 35. Maturing Von Mises stress field for interphases 0.1mm (Top Left), 0.3mm (Top Right) and 0.4mm (Bottom) with a 0.7mm LEP.

5.4 Interphase – 0.1mm (LEP – 0.3, 0.5, 0.7 mm)

Previously, the interphases were observed for a constant LEP thickness which helped understand the influence of interphase thickness on the resultant stress field. In order to design an optimized LEP solution, it is also important to understand how the LEP thickness influences the stress field to develop a holistic understanding of the interactions between the LEP-substrate system while considering the interphase.

Figure 36 compares the stress field of a 0.1mm interphase for varying LEP thicknesses. The influence of LEP thickness on the stress field is distinctly visible. In the 0.3mm LEP, the stress is concentrated with the highest amplitude of 14 MPa across the interphase region, while transitioning between the LEP-interphase and interphase-substrate regions respectively. An additional stress concentration is observed at the surface of the LEP of amplitude 10 MPa. The stress concentration in the 0.5mm and 0.7mm LEP's are distinct with an observable stress concentration banded region in the LEP. In the 0.5mm LEP, the stress concentration across the interphase region is lower in amplitude, 8.2 MPa compared to the 0.3mm LEP, 14 MPa. This stress concentration transitions into the substrate as can be seen. The stress in the 0.7mm LEP is lightly concentrated with lower amplitudes of stress, 7.5 MPa, with the banded stress concentration region in the LEP still visible. The stress across the interphase decreases with a thicker LEP as the stress is concentrated at the surface and is absorbed by the LEP while being supported by the substrate. For the LEP thicknesses studied, the stress field observed are visibly different but have similar stress states, which have high stress concentrations. This highlights the influence of LEP thickness the developing stress field.

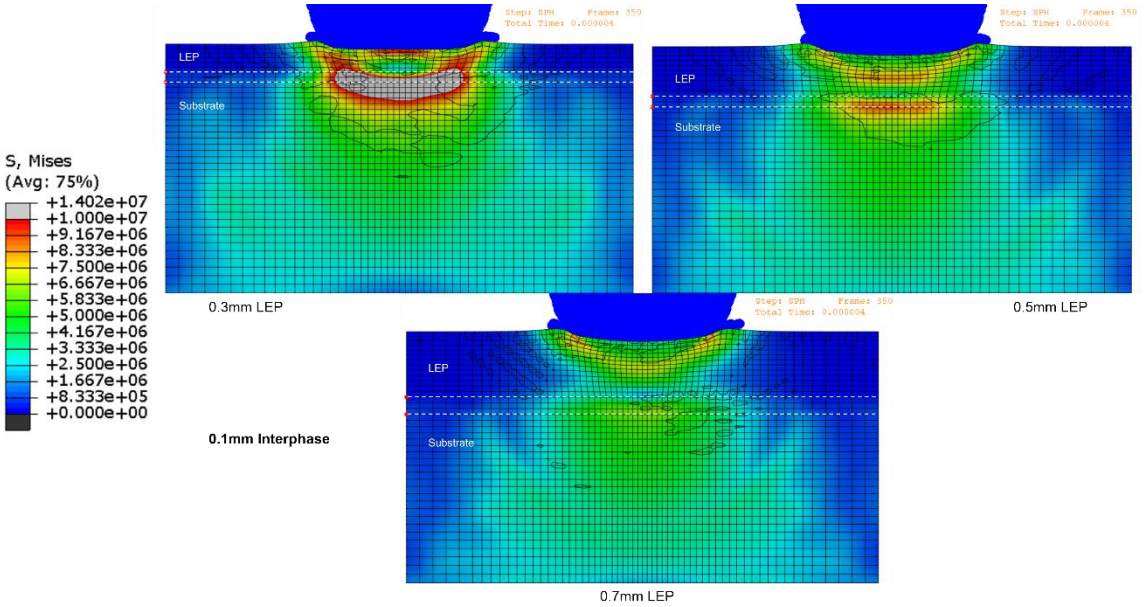

Figure 36. Von Mises stress field for 0.1mm interphase with varying LEP's (0.3mm (Top), 0.5mm (Middle), 0.7mm (Bottom))

5.5 Interphase – 0.3mm (LEP – 0.3, 0.5, 0.7 mm)

Figure 37 shows the stress field observed for a 0.3mm interphase. Akin to the previous analysis, the stress fields in the LEP's depict a progression with the 0.3mm LEP representing a closely matured final state, while the 0.5 and 0.7mm LEP's show the progression of the stress fields toward the latter. Though the stress fields for the LEP's resemble the 0.1mm interphase system, the amplitude of stress observed is lower (10.77 MPa). This is especially seen across the interphase regions in the different LEP systems, where the stress concentrations and amplitudes are reduced compared to the 0.1mm interphase system. Here, the superficial stresses in the 0.5mm and 0.7mm LEP's are relatively higher, signifying that the location of damage initiation, could propagate from these regions with observable surface indentations in a fatigue mechanism. Whereas, in the 0.3mm LEP, the Internal and superficial stresses are balanced. The overall wavefront observed is smoother, continuous, and more rounded compared to the 0.1mm interphase.

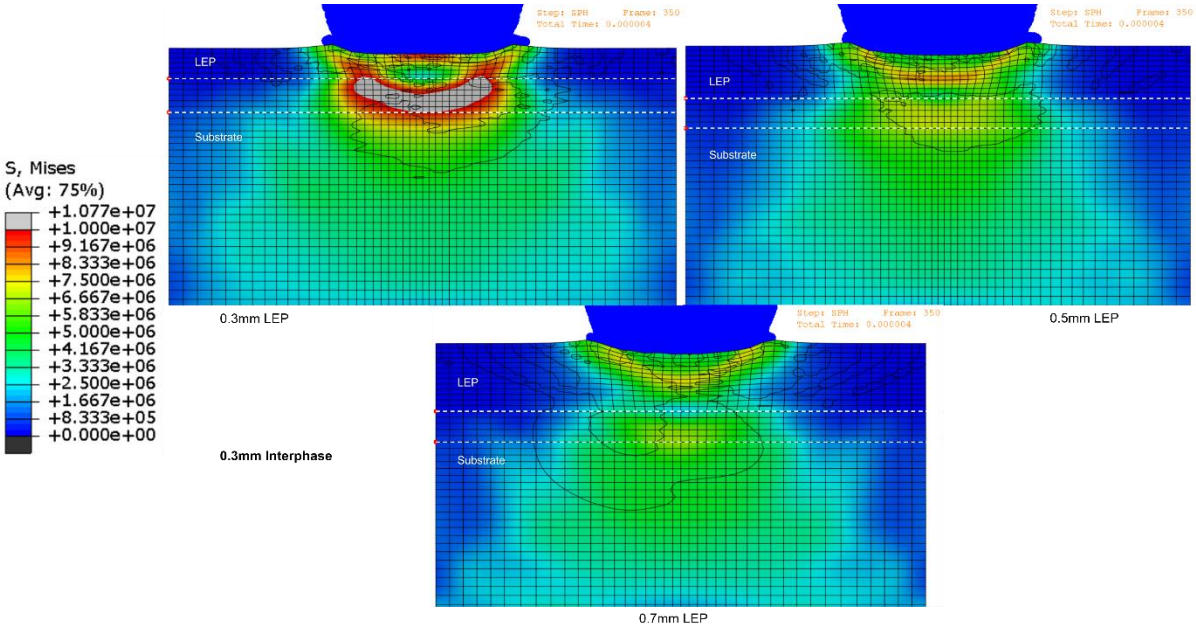

Figure 37. Maturing Von Mises stress field for the 0.3mm interphase with varying LEP thicknesses (0.3mm (Top Left), 0.5mm (Top Right), 0.7mm (Bottom))

5.6 Interphase – 0.4mm (LEP – 0.3, 0.5, 0.7 mm)

The stress field observed for a 0.4mm interphase is shown in Figure 38. The amplitude of stresses observed is lower and the overall wavefronts are smooth and continuous. The stress concentration across the interphase region for the 0.3mm LEP is relatively compact as compared to the previous interphase systems. This could result from the increased interphase thickness. The stress across the interphase is comparatively lower, with reduced amplitudes of stress across the banded region in the LEP's (Approximately 10% reduction in stress amplitudes). For a viable LEP solution, a thicker LEP reduces the impact of the stresses transmitted into the substrate due the impedance of the LEP and substrate. However, an optimal interphase thickness that compliments the selected LEP thickness would need to be optimized further.

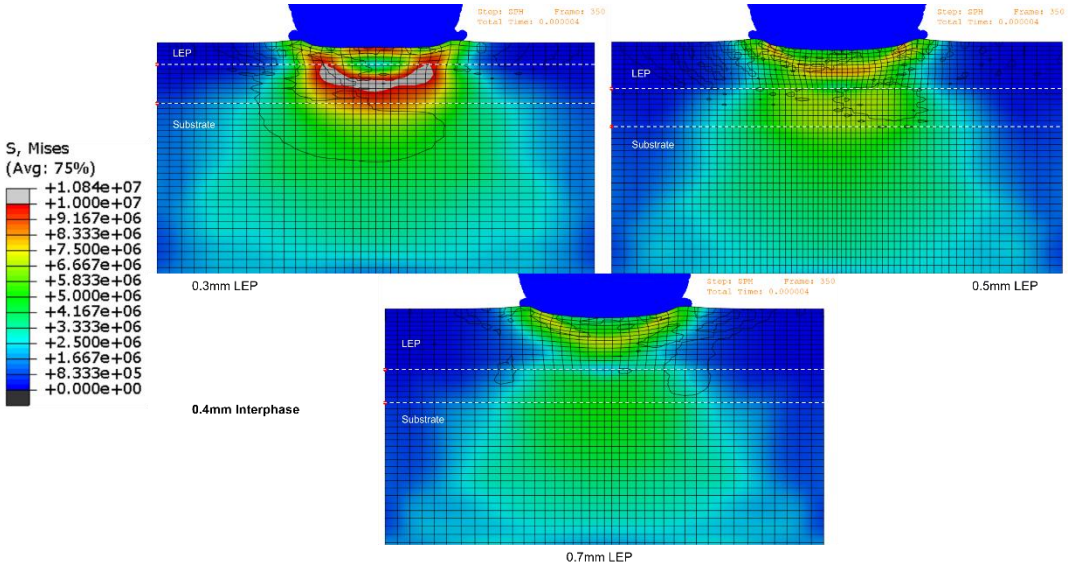

Figure 38. Maturing Von Mises stress field for 0.4mm interphase with varying LEP's (0.3mm (Top Left), 0.5mm (Top Right), 0.7mm (Bottom))

5.7 Summary

In this chapter, the influence of an interphase region on the stress field was discussed. The interphase region had a linear transition in material properties between the LEP and substrate, and was modeled using Functionally Graded Materials, which was discussed in Chapter 2. Furthermore, the influence of LEP thickness on the interphase and stress field was discussed. Two stress states observed at 1.75 and 3.50 microseconds, respectively were studied for varying LEP and interphase thicknesses.

It was observed that for thinner LEP's, the amplitude of stress across the interphase region was greater than for thicker LEP's. This is partly due to the stress field in thinner LEP's maturing faster than in thicker LEP's. Additionally, in thicker LEP's the energy density in the waves is lower when it reaches the interphase region. A banded stress concentration region in the LEP is observed in the system studied, which is caused by the impedance between the LEP-interphase and interphase-substrate regions respectively.

Similarly, for thinner interphases it was observed that the amplitudes of stress were greater than for thicker interphases. This is due to the rapid change in material properties for thinner interphases, while the transition in material properties is gradual for thicker interphases. This results in a lower stress region above the observable stress concentration region. This is caused by the inertia of the propagating waves in the system across the interphase region.

A key observation from the interphase simulations is the co-dependence of material properties on the LEP thickness and corresponding interphase thickness. Identifying such a solution will help define design guidelines for an optimize co-bonded LEP solution. An optimal solution would be a larger interphase thickness with the least amplitude of stress as this would reduce the possibility of delamination and debonding at the interphase region.

Chapter 6 : Optimized LEP solution

When optimizing an LEP solution, it is important to understand the wave propagation through the system and, the type of damage and location of damage initiation in the system. This chapter highlights the differences between a discrete interface and interphase while looking at the maximum stress in each system. To optimize the performance of a given LEP system, the maximum stress needs to be considered, since damage initiates at this instance.

6.1 Discrete Interface vs. Interphase

LEP coatings are typically bonded to the substrate with the help of adhesives or are co-bonded during the manufacturing process. These methods of bonding are studied as the discrete interface and interphase, respectively. To design and optimize a viable LEP solution, understanding the differences between a discrete interface and interphase in terms of damage mechanisms is discussed in this section where the focus lies on TPU A80.

Figure 39 shows the discrete interface treated as an interphase region of 0mm thickness where, the influence of maximum stress on the stress field can be compared. The maximum stress occurs at 3.86 microseconds as shown in Table 5. The 0.1mm interphase has the highest amplitude of stress at 8.8 MPa, caused by rapid change in material properties resulting in earlier reflections in the system. Likewise, the lowest amplitude of stress is observed in the 0.4mm and 0.5mm interfaces as 8 MPa. Comparing this to the discrete interface or 0mm interphase, the maximum amplitude of stress is 8.6 MPa with a banded stress concentration in the center of the LEP. This banded region is observed in the interphases as well and is caused by the reflections in the system yielding from the interaction of the compressional and tensile waves in the LEP.

Since the amplitudes of stress for the 0mm, 0.1mm and 0.3mm interphases are comparable with similar observable instances, the effect of transitioning material properties on the stress field remains consistent. This suggests that the internal and superficial stresses for this LEP thickness are equal, indicating damage initiation either at the center or surface of the LEP. Therefore, the damage initiation and wave propagation for the discrete interface and interphases of similar LEP thicknesses are comparable. The wavefront observed in the discrete interface and interphases are different due to the linear transition in material properties at the interphase. This results in a smooth and continuous wave front between the LEP and substrate. Additionally, as the interphase thickness increases, the wavefront develops gradually and smoothly. This could play an important part in identifying the internal stress development in the substrate to optimize and predict a corresponding suitable LEP.

Table 5. Maximum stress at interphases for a 0.7mm TPU A80 LEP.

Interphase thickness (mm)	LEP thickness (mm)	Instance (microseconds)	Maximum stress (MPa)
0.0 (Discrete)	0.75	3.86	8.6
0.1	0.7		8.8
0.3			8.7
0.4			8
0.5			8

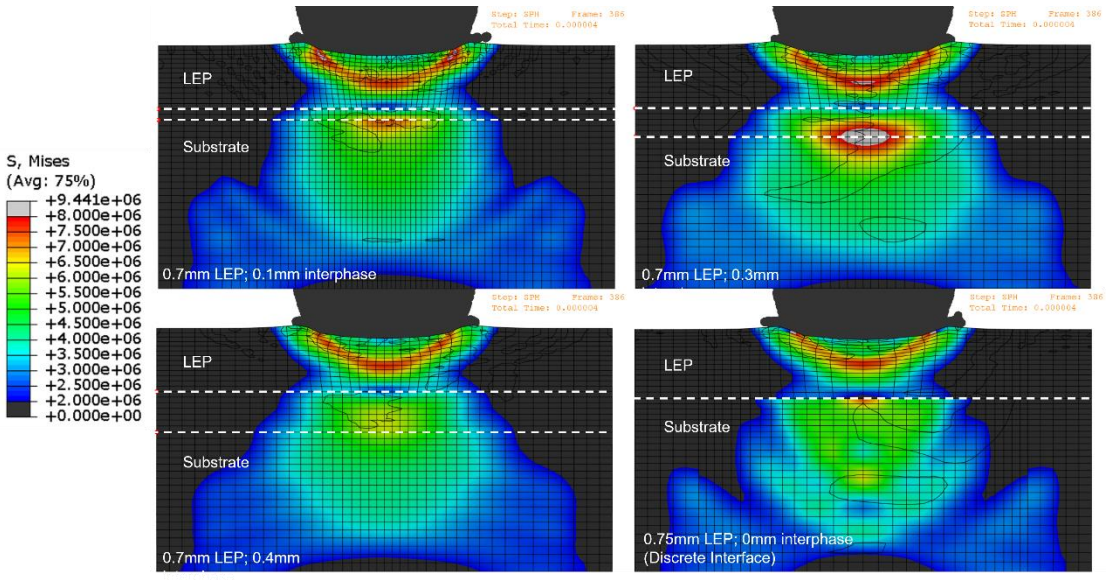

Figure 39. Maximum stress in the 0.7mm LEP for interphases - 0.1mm (Top Left), 0.3mm (Top Right), 0.4mm (Bottom Left), and 0mm (Bottom Right) (Discrete Interface).

6.2 TPU D60

Analyzing the discrete 0.25mm and 0.5mm LEP's for TPU D60 as shown in Figure 40. The maximum stress in the 0.25mm LEP is 30 MPa observed at 0.83 microseconds, while for the 0.5mm LEP the same is observed at 0.79 microseconds as 33 MPa. In both these LEP's the stress is concentrated at the surface of the LEP indicating damage initiation in the LEP for a fatigue mechanism. For the 0.25mm LEP, reflections in the system are observed at the interface, which increases the stress concentration in the LEP although the amplitude of the reflected wave is lower in comparison to the compressional wave. Calculating the modified water hammer pressure for TPU D60 yields a value of 60.44 MPa, which is an analytical approximation of the contact pressure developed upon droplet impact. This high contact pressure coupled with the intrinsic material properties of TPU D60, results in stress concentrations at the surface of the LEP. This suggests that the superficial stresses in these systems are the dominant mechanisms of damage compared to the internal stresses, since the location and instances when the maximum stress is observed for the two LEP thicknesses are comparable despite the variation in the respective stress fields.

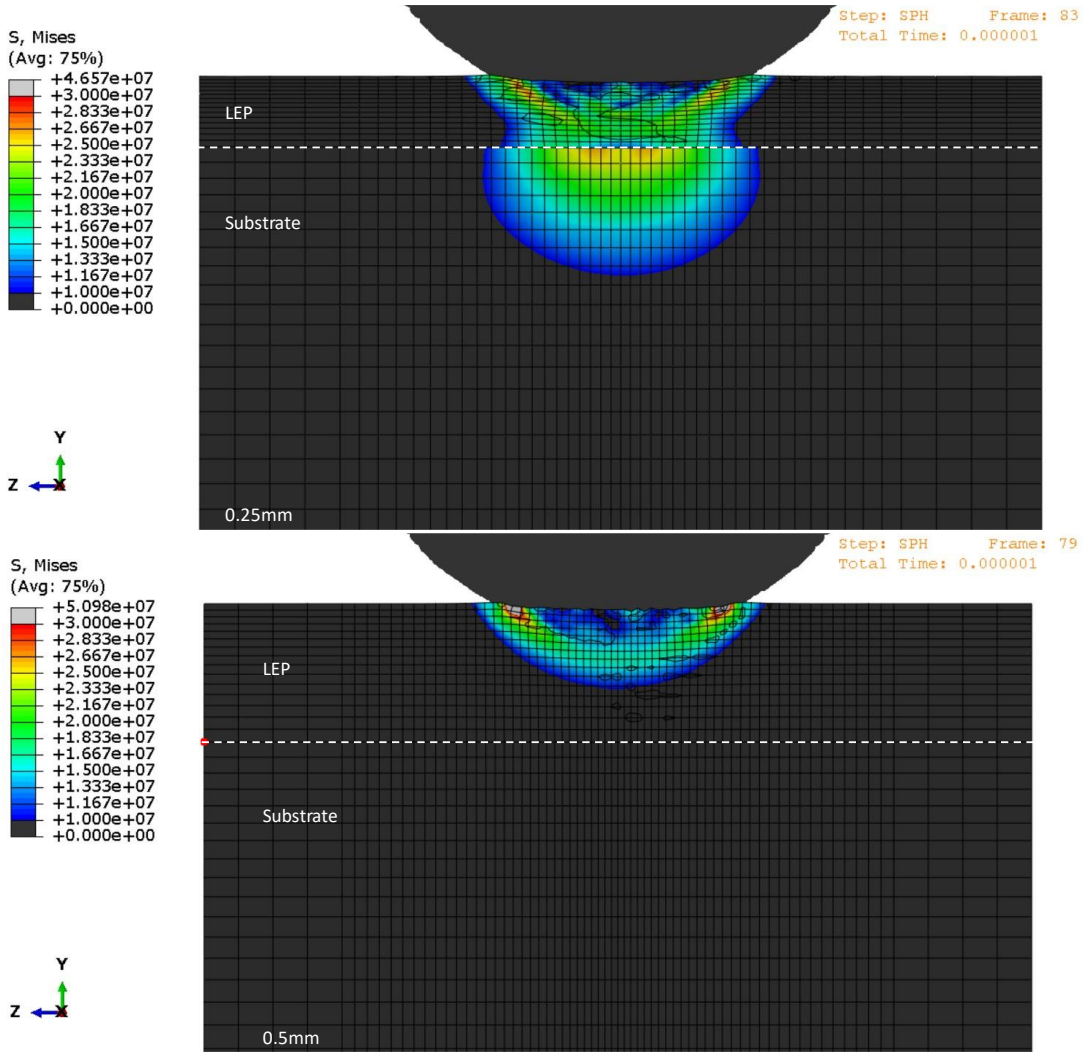

Figure 40. Von mises stress field showing the maximum stress for the 0.25mm (Top) and 0.5mm (Bottom) LEP's (TPU D60).

The 0.75mm LEP has a maximum stress amplitude of 33 MPa observed at 0.81 microseconds, while the 1.0mm LEP has an amplitude of 32 MPa observed at 0.87 microseconds as shown in Figure 41. Like the previous LEP thicknesses studied, the superficial stress at the surface of the LEP results in a stress concentration of relatively lower amplitude, where damage initiates under a fatigue mechanism. The stress is yet to transmit into the substrate, suggesting this is partly because the impact energy is dissipated by the LEP and the wave requires longer to travel the additional LEP thickness. For the 0.75mm and 1.0mm LEP thicknesses, the damage location and instance of damage are similar to the 0.5mm LEP, whose system yields similar results with less LEP thickness (material required). Therefore, a viable and desirable LEP solution would be to implement the 0.5-0.75mm LEP for TPU D60.

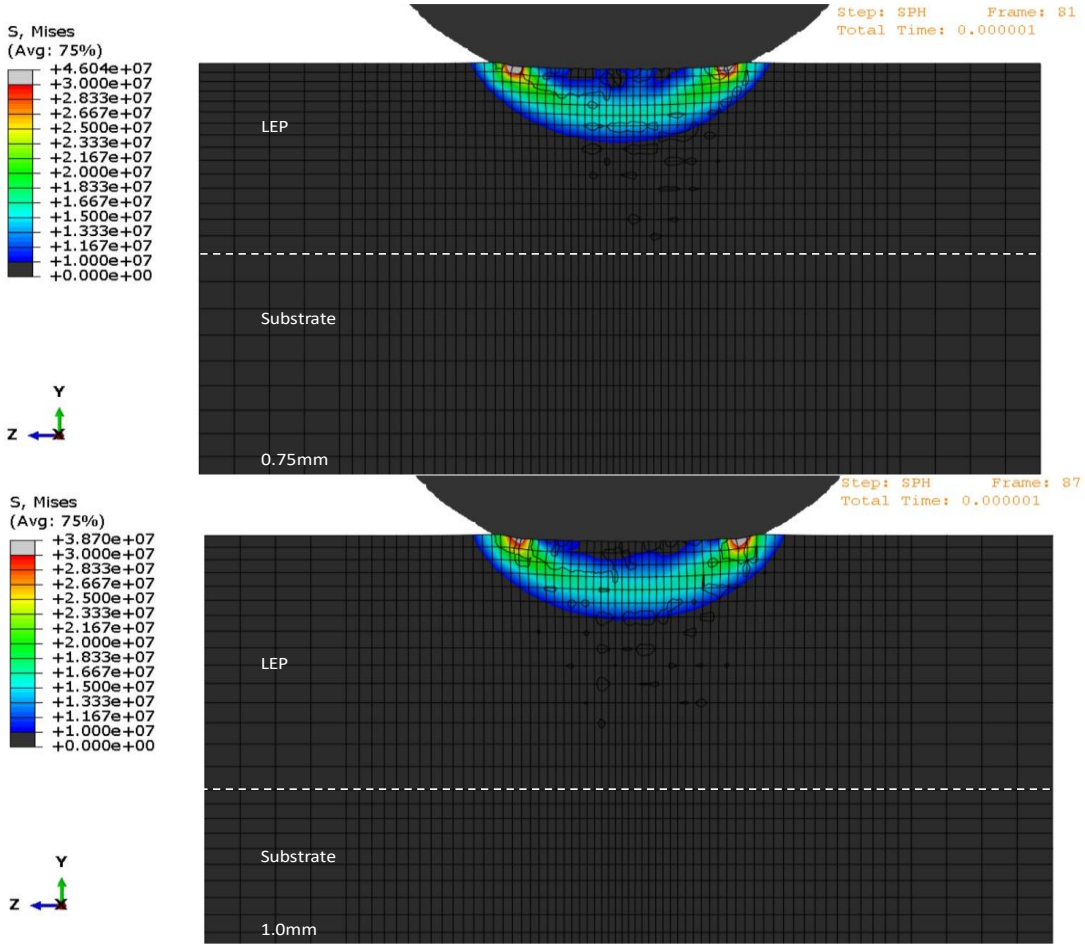

Figure 41. Von mises stress field showing the maximum stress for the 0.75mm (Top) and 1.0mm (Bottom) LEP's (TPU D60).

6.3 TPU A80

The maximum amplitude of stress in the 0.25mm LEP is observed at 2.94 microseconds as 13.7 MPa in the LEP, while for the 0.5mm LEP it is observed at 3.30 microseconds as 9 MPa in the LEP. Figure 42 shows the maximum stress in the LEP is observed at a later period compared to TPU D60 since TPU A80 is compliant has a lower approximated contact pressure of 49.76 MPa. For the 0.25mm LEP, the stress concentration observed at the interface is caused by reflections in the LEP, hence, occurring at a later period. While the stress at the surface of the LEP is caused by the high energy density of the compressional wave induced upon droplet impact. However, due the inherent material characteristics of TPU A80 and epoxy, the induced waves propagate at different speeds within the LEP and substrate, dispersing faster in the substrate. Thus, the stress concentrations in the LEP develop towards the center of the LEP, suggesting the development of internal stresses followed by superficial stresses in the LEP. In the 0.5mm LEP a stress band in developed in the LEP, highlighted as a yellow band possessing an amplitude of 8.5 MPa. This stress band culminates in internal stresses in the system which occur earlier than the superficial stresses, indicating damage initiation begins at the center of the LEP. This LEP thickness highlights the lower limit wherein the internal stresses are higher than the superficial stresses in the system.

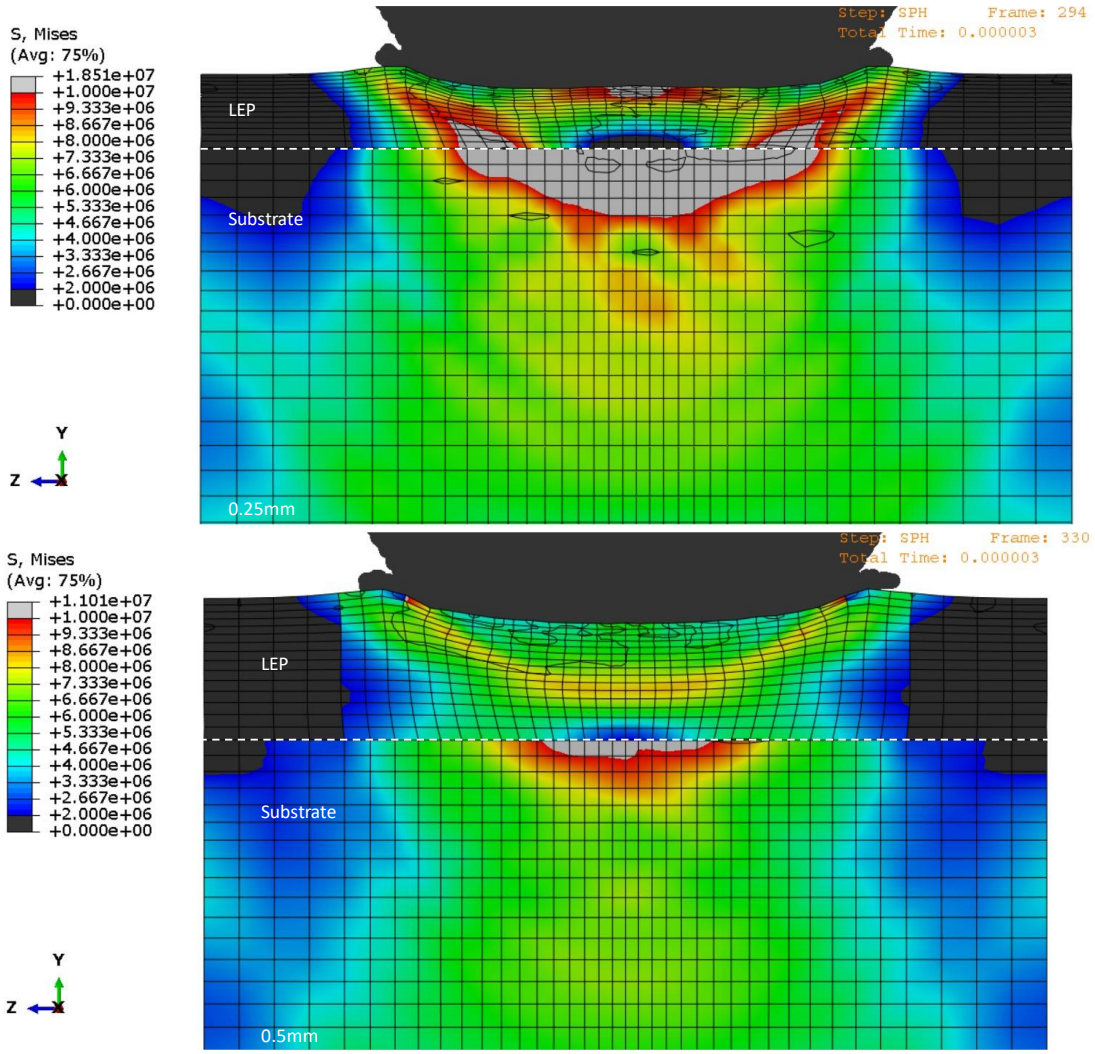

Figure 42. Von mises stress field showing the maximum stress for the 0.25mm (Top) and 0.5mm (Bottom) LEP's (TPU A80).

In the 0.75mm and 1.0mm LEP's, the maximum amplitudes of stress are observed at 3.86 microseconds as 8.6 MPa and 7.8 MPa, respectively. Figure 43, shows the stress concentration in the 0.75mm LEP observed at the center and surface of the LEP possessing equal amplitudes of stress. This suggests that the superficial and internal stresses in the 0.75mm LEP are equal, indicating damage could initiate at either the surface or center of the LEP. This LEP thickness is unique since it represents the lower limit at which superficial stresses occur and the upper limit, beyond which the superficial stresses would dominate internal stresses in damage propagation as observed in the 1.0mm LEP. In the 1.0mm LEP, the stress is concentrated at the surface of the LEP. This is the point of damage initiation, confirming superficial stresses to be dominant in this system which result in damage under a fatigue mechanism. The 1.0mm LEP highlights the limit at which the LEP shields the substrate effectively as having a thicker LEP would result in superficial stresses, where the stress concentrations are no longer dependent on the reflections in the system. Thus, the maximum stress would remain the same for LEP's thicker than 1.0mm. Although the 1.0mm has a lower amplitude of stress, the 0.75mm shields the substrate effectively while requiring a reduced LEP thickness. Since the 0.75mm LEP shields the substrate with a reduced LEP thickness, compared to the 1.0mm LEP, it shows a promising LEP solution for TPU A80.

(Note: In the 0.75mm LEP, the maximum stress at the surface of the LEP are confined to a single node. This is a numerical error and should be considered as the stress propagation is predictable. This error can be addressed by refining the mesh further. However, this is not done here since the standard model had to remain comparable for different materials)

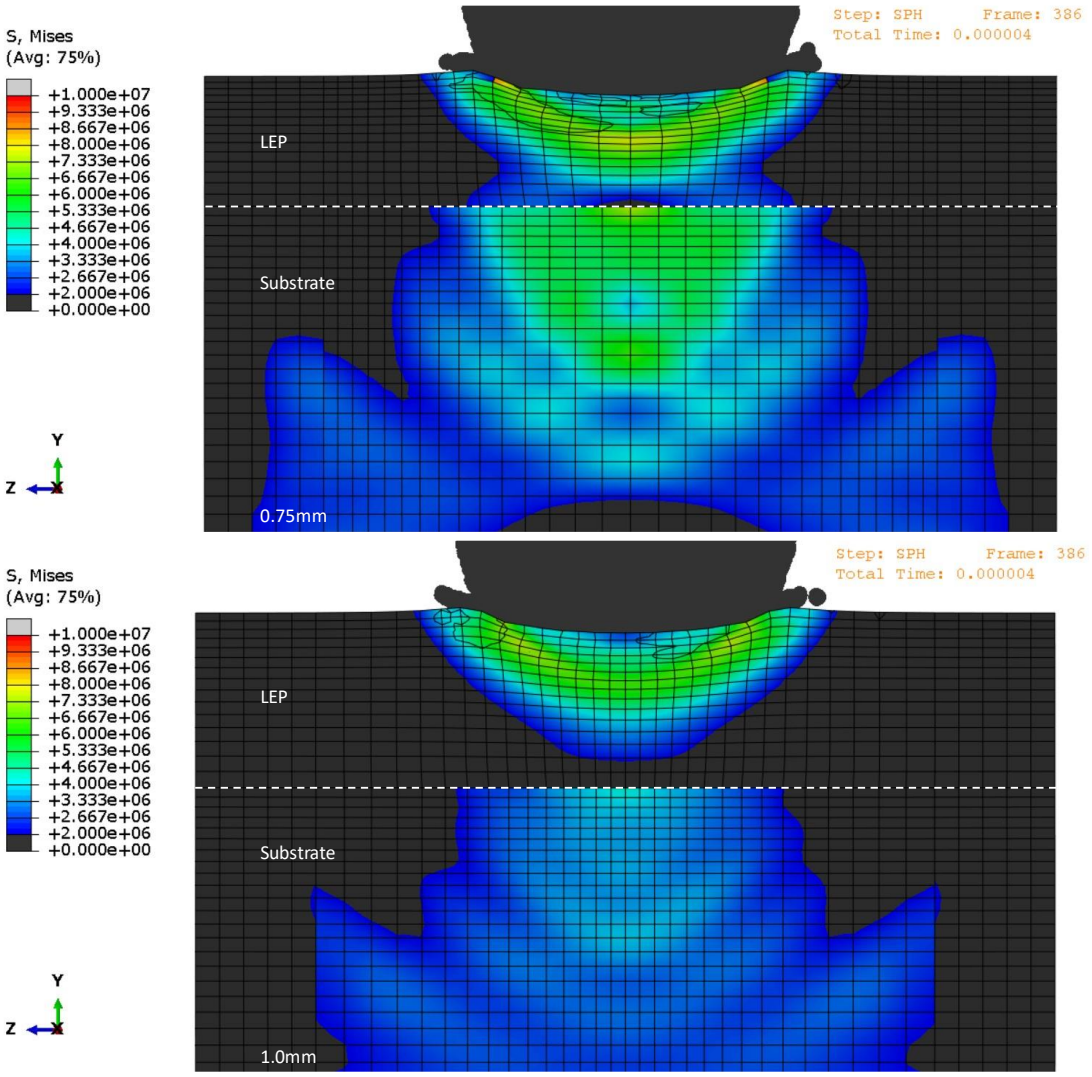

Figure 43. Von mises stress field showing the maximum stress for the 0.75mm (Top) and 1.0mm (Bottom) LEP's (TPU A80).

6.4 ABS

ABS has highest approximated contact pressure observed for the studied LEP's at 75.07 MPa. The maximum amplitude of stress for the 0.25mm and 0.5mm LEP's are observed at 0.30 microseconds and 0.32 microseconds as 60 MPa and 58 MPa, respectively as shown in Figure 44. For both LEP's superficial stresses are present which will ultimately lead to fatigue damage. Additionally, since ABS and epoxy have similar properties, the impact energy is dissipated through the LEP and substrate functioning as a single system. Therefore, thinner LEP's like the 0.25mm and 0.5mm show promising results for ABS.

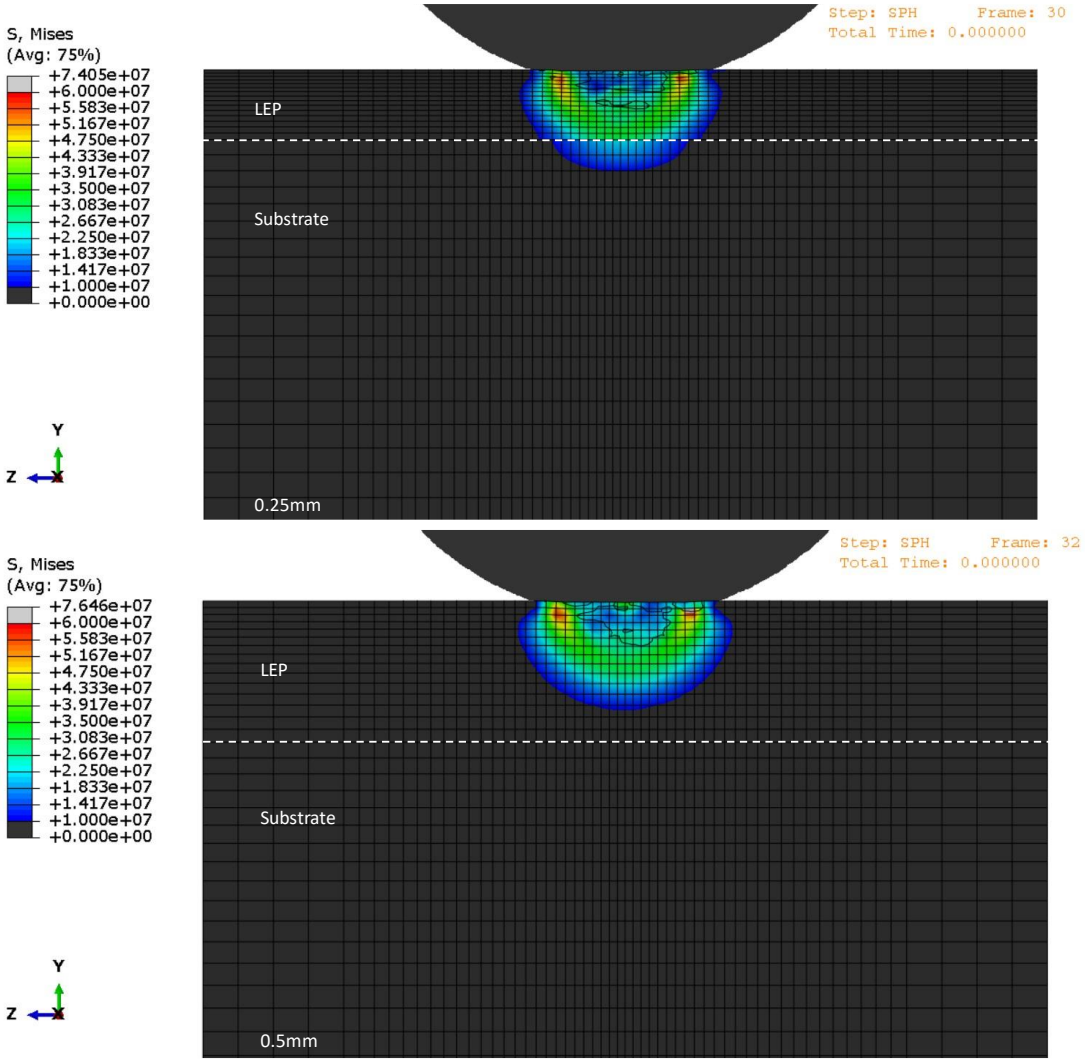

Figure 44. Von mises stress field showing the maximum stress for the 0.25mm (Top) and 0.5mm (Bottom) LEP's (ABS).

For the 0.75mm and 1.0mm LEP's the maximum stress is observed at 0.37 microseconds and 0.30 microseconds as 51 MPa, respectively as shown in Figure 45. In both these LEP's damage initiation is driven by superficial stresses as the internal stresses are negligible. Since the 0.5mm LEP shields the substrate from damage with less LEP thickness (less material), thinner LEP's like the 0.25mm and 0.5mm are preferred over the 0.75mm and 1.0mm LEP's as viable LEP solution for ABS.

(Note: The stress fields observed for ABS are similar in all the cases, however, the variation in stress values is peculiar. This could be due the mesh definition in the standard model. A refined mesh definition could yield uniform stress values.)

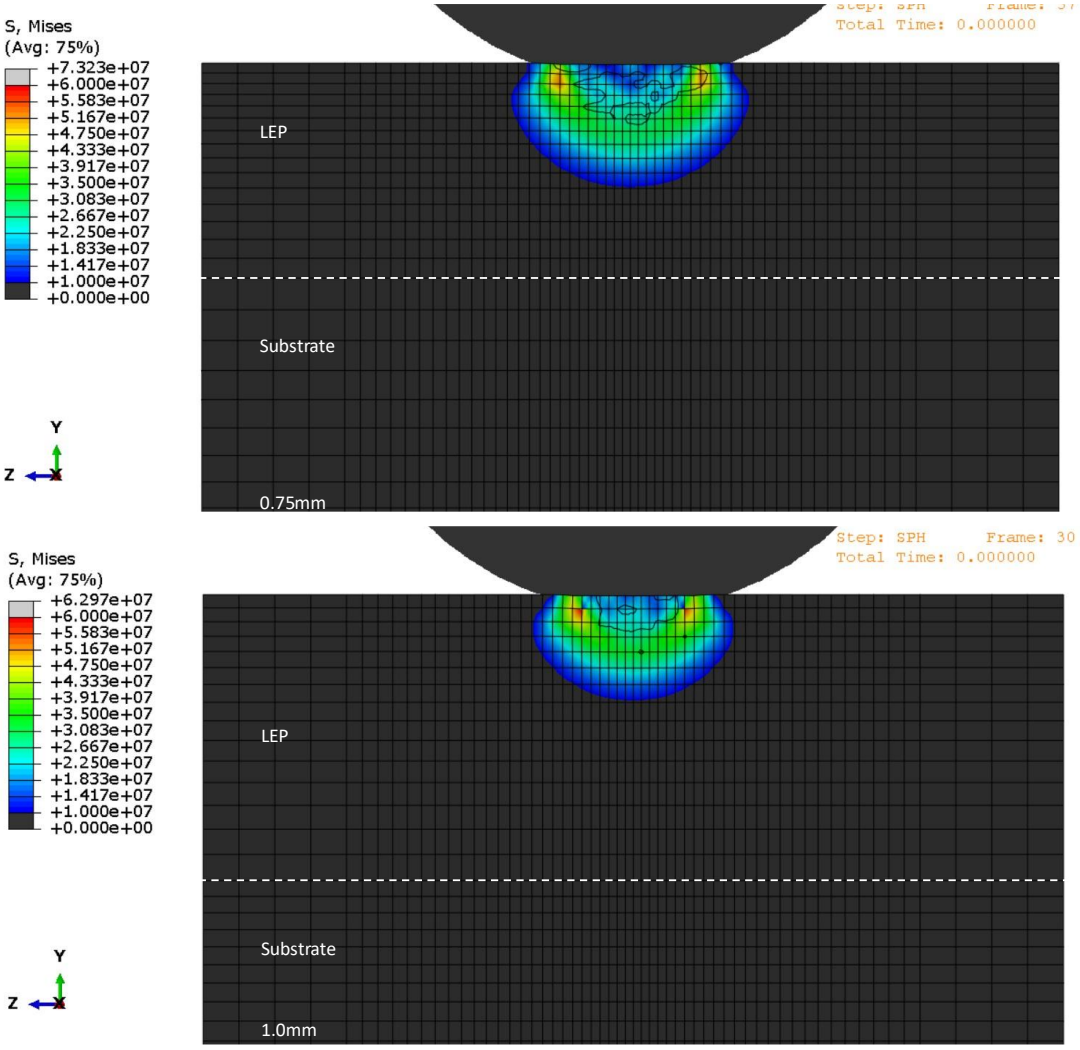

Figure 45. Von mises stress field showing the maximum stress for the 0.75mm (Top) and 1.0mm (Bottom) LEP's (ABS).

6.5 Design Guidelines

In this chapter the differences between the discrete interface and interphase were discussed along with the maximum stresses in each LEP which highlight the dominant damage mechanisms in the system. This provides insights into a viable LEP solution for each LEP material studied. Table 6, provides an overview of the maximum stresses in the LEP's along with the instance at which it occurs. The highlighted LEP thicknesses correspond to the most promising results for that material. The factors that govern these results can be extrapolated as material related design guidelines for the development of a LEP solution.

Table 6. Maximum stress amplitudes observed in discrete LEP's.

LEP material	Maximum stress state (microseconds)	LEP thickness (mm)	Maximum stress amplitude (MPa)
TPU D60	0.83	0.25	30
	0.79	0.5	33
	0.81	0.75	33
	0.87	1.0	32
TPU A80	2.94	0.25	13.7
	3.30	0.5	9
	3.86	0.75	8.6
	3.86	1.0	7.8
ABS	0.30	0.25	60
	0.32	0.5	58
	0.37	0.75	51
	0.30	1.0	51

For stiffer materials like TPU D60 and ABS, the superficial stresses result in damage initiation. Additionally, the amplitude of stress observed in ABS is relatively high due to its higher Young's Modulus compared to TPU D60. Contrary to stiff materials, compliant materials like TPU A80 have a lower amplitude of maximum stress which occurs at a later period. This results in internal and superficial stresses in the LEP based on the thickness of the LEP. Given the low Young's Modulus of TPU A80 compared to the epoxy substrate, the stress is initially dispersed in the substrate and subsequent reflections in the system result in stress in the LEP.

Therefore, from these factors and material characteristics, the following design guidelines can be derived:

- For stiffer materials like ABS and TPU D60, thinner LEP's provide the best results. Such as the 0.25mm and 0.5mm LEP's for ABS and 0.5mm LEP for TPU D60.

- For compliant materials such as TPU A80, thicker LEP's like the 0.75mm LEP where the dominant stress changes from internal to superficial stresses, provides the best results.

- Stiffer materials typically have higher amplitudes of stress concentrated along the surface of the LEP resulting in superficial damage.

- Compliant materials, have lower amplitudes of stress concentrated along the surface and center of the LEP. Suggesting that the internal and superficial stresses in the system are equal. Therefore, damage could initiate at either the surface or internally in complaint LEP depending on the thickness of the LEP used.

- In stiffer materials, the induced compressional waves have a high energy density that propagates the stress concentration, while in compliant materials, the stress concentrations are driven by the reflections in the system.

- When co-bonding LEP's to substrates, a thicker interphase region has a gradual transition in material properties with lower amplitudes of stress. While thinner interphase regions have a faster transition in material properties where the stress field develops early on and has higher amplitudes of stress.

- In the interphase regions, a low stress concentration region is observed above the stress concentration in the interphase region. This is due to transition in material properties which affects the inertia of the propagating stress wave. For thicker interphase regions this is minimal.

- The influence of LEP thickness on the stress field despite the discrete interface or interphase is dependent on the material properties of the system.

- Considering the material properties of the substrate to complement the selected LEP results in optimal usage of material characteristics of the system where the LEP implemented can be of optimal thickness.

Implementing the derived design guidelines, an instance for an optimized LEP solution for TPU A80 with a continuous interphase thickness of 0.4mm for an LEP thickness of 0.7mm is shown in Figure 46. Here, the optimized substrate has a central mesh with 30 elements and 40 elements in the thickness coordinate. Whereas the droplet has 130 elements in the lower region and 40 elements around its circumference. The resultant stress field observed is gradual with minimal stress across the interphase, while the LEP effectively shields the substrate.

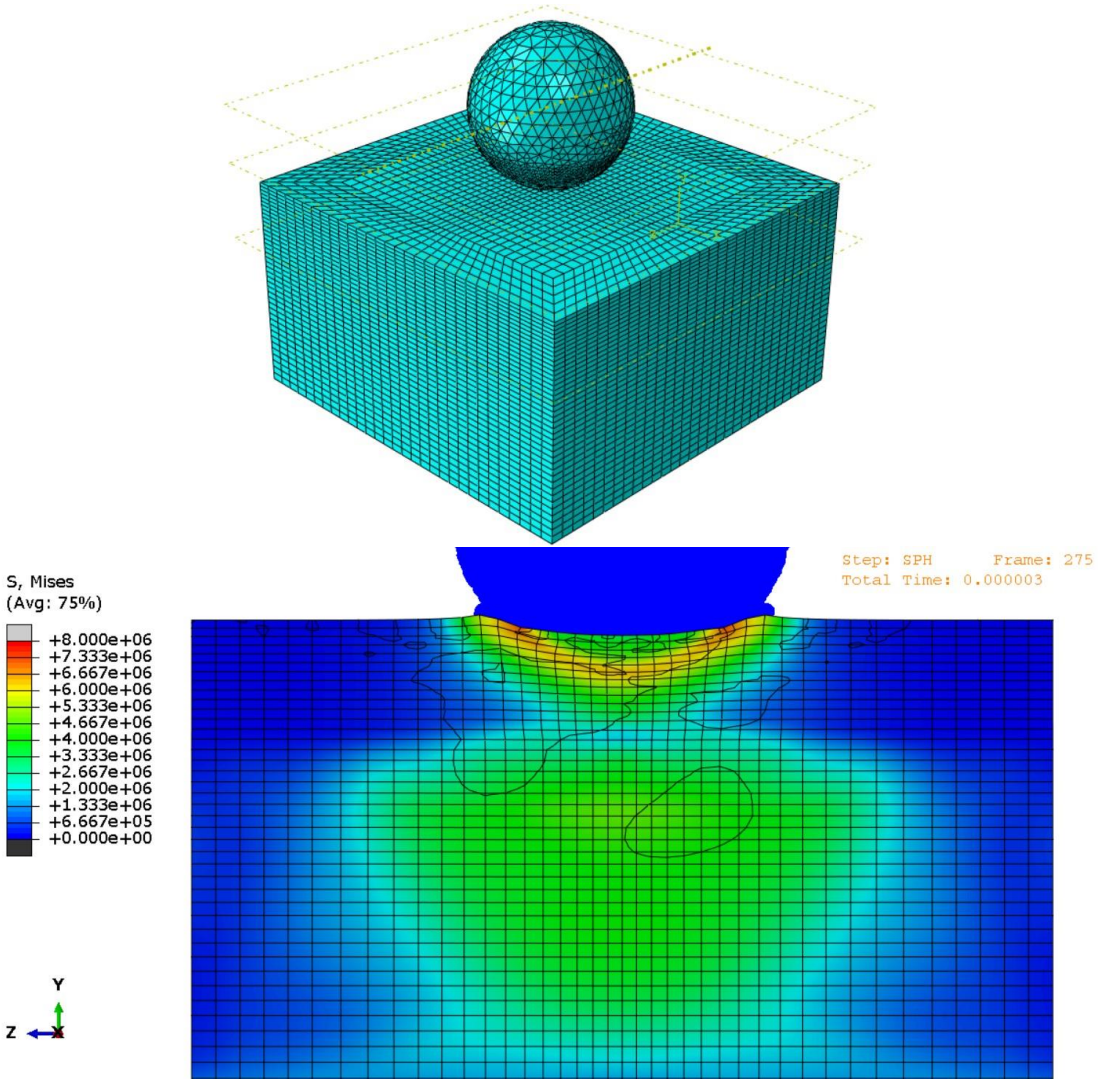

Figure 46. Optimized TPU A80 LEP solution showing the optimized mesh and resultant stress field for a continuous interphase (0.4mm -interphase; 0.7mm LEP).

Chapter 7 : Conclusions

Offshore wind farms are crucial in the transition towards renewable energy. Having the highest potential, offshore wind turbines are increasing in size to maximize outputs. An adverse effect of this process is the exponential erosion rates observed due to the higher tip speeds in excess of 100 m/s. This assignment strives to provide a suitable leading edge protection solution to shield the turbines from rain erosion. Thermoplastic LEP's studied in this assignment are ABS, TPU D60 and TPU A80. The following research questions have been tackled in this assignment to design an optimized LEP solution.

- **How does the wave propagate in a multilayered substrate for different LEP materials?**

  Upon droplet impact, a compressional wave is induced in the LEP which is transmitted and reflected according to the impedance of the system. This results in a reflected 'tensile' wave in the LEP and a transmitted wave in the substrate. Upon impact in addition to the compressional wave, a shear wave is induced in the system. The interaction of these waves results in superficial or internal stresses in the system dependent on the material properties of the LEP and substrate.

- **How does LEP thickness influence the stress field for different LEP materials?**

  The simulations show a direct correlation between the LEP thickness and stress in the system, where the stress in the system is inversely proportional to the thickness of the LEP. Owing to the high energy density of the induced compressional waves, thinner LEP's dissipate the energy less before being transmitted into the substrate. This results in the earlier development of the stress field as opposed to thicker LEP's. Additionally, depending on the intrinsic material properties of the system, stress concentrations and wave propagation in the system differ for compliant and stiff materials.

- **How does an interphase influence the stress field?**

  The insights provided from the above-mentioned discrete interface simulations, provide the framework for analysis of the interphase between the LEP and substrate. The interphase is a region of linearly transitioning material properties between the LEP and substrate. Hence, the wavefront developed is smoother and continuous compared to the discrete interface. The thickness of the LEP and interphase affect the stress field due to the rapid transition of material properties in thinner interphases leading to early development of the matured stress state.

- **What mechanisms/parameters are important for LEP performance?**

  For each material studied a promising LEP thickness based on the wave propagation, material properties and predicted damage mechanisms has been identified. (TPU D60 – 0.5mm; TPU A80 – 0.75mm; ABS – 0.25mm, 0.5mm) Extrapolating the material properties of the LEP's studied enables an extraction of design guidelines for materials based on their inherent properties. These are discussed in section 6.5 Design Guidelines.

7.1 Recommendations:

The materials used as LEP coatings have unique properties and characteristics. Hence, developing or optimizing singular materials is difficult as this cannot be adopted to other materials. Therefore, this thesis derived guidelines that could be adopted to a range of materials, both stiff and compliant in nature as each has its own unique application. The research and results in this thesis can be further investigated and tested to improve the derived LEP solution. The recommendations suggested are as follows:

- The mesh can be further refined to obtain detailed stress fields. The mesh in this thesis is refined to accommodate the standard model with the LEP materials. Further refining of the mesh would yield numerical errors for a few simulations and increase the computational time.

- Using the substrates' properties along with the designed LEP, ensures optimal LEP thickness and utilization of material properties. ABS and epoxy is one such example, wherein the LEP and substrate have similar properties and function as a single layer. This has been tested in the industry in the application of gelcoats.

- Testing the suggested LEP thickness for materials with Rain Erosion Testing (RET) would help plot the lifecycle of the specimen against the predicted lifecycle of the specimen using fatigue theory. This would also validate damage initiation.

- Conducting microscopy to study and analyze the interphase would help identify and validate the influence of interphase thickness on the stress field/ system.

- Polycarbonates and Aluminium would make good LEP's due to their high strength properties and superficial damage. Preliminary investigations are shown in APPENDIX B.

Bibliography

[1] "Wind energy in Europe 2020 Statistics and the outlook for 2021-2025," [Online]. Available: https://windeurope.org/intelligence-platform/product/wind-energy-in-europe-in-2020-trends-and-statistics/#presentations.

[2] "Wind energy today," [Online]. Available: https://windeurope.org/about-wind/wind-energy-today/.

[3] "Offshore Wind Outlook 2019," [Online]. Available: https://www.iea.org/reports/offshore-wind-outlook-2019.

[4] M. Keegan, "Wind Turbine Blade Leading Edge Erosion: An investigation of rain droplet and hailstone impact induced damage mechanisms," 2014.

[5] L. Rempel, "Rotor blade leading edge erosion-real life experiences.," *Wind Systems Magazine,* vol. 11, pp. 22-24, 2012.

[6] L. Bartolomé and J. Teuwen, "Prospective challenges in the experimentation of the rain erosion on the leading edge of wind turbine blades.," *Wind Energy,* vol. 22, p. 140– 151, September 2019.

[7] "VATTENFALL AND GE JOIN FORCES TO DEPLOY HALIADE-X 12MW WIND TURBINE," [Online]. Available: http://www.energyglobalnews.com/vattenfall-and-ge-join-forces-to-deploy-haliade-x-12mw-wind-turbine/.

[8] R. Jonsson, "Characterisation and Validation of a Pulsating Jet Erosion Test," vol. 279, 2007.

[9] E. Cortés, F. Sánchez , A. O'Carroll, B. Madramany, M. Hardiman and T. M. Young, "On the Material Characterisation of Wind Turbine Blade Coatings: The Effect of Interphase Coating–Laminate Adhesion on Rain Erosion Performance," *Materials,* vol. 10, p. 1146, September 2017.

[10] T. Hoksbergen, I. Baran and R. Akkerman, "Rain droplet erosion behavior of a thermoplastic based leading edge protection system for wind turbine blades," *IOP Conference Series: Materials Science and Engineering,* vol. 942, October 2020.

[11] M. Elhadi Ibrahim and M. Medraj , "Water Droplet Erosion of Wind Turbine Blades: Mechanics, Testing, Modeling and Future Perspectives.," *Materials,* vol. 13, p. 157, 2020.

[12] A. Verma, "Leading edge erosion of wind turbine blades: Effects of blade surface curvature on rain droplet impingement kinematics," *J. Phys.: Conf. Ser. 1618 052003,* vol. 1618.

[13] M. Keegan, D. Nash and M. Stack, "Modelling Rain Drop Impact of Offshore Wind Turbine Blades," *Proceedings of the ASME Turbo Expo,* vol. 6, 2012.

[14] E. Tobin, T. Young, D. Raps and O. Rohr, "Comparison of liquid impingement results from whirling arm and water-jet erosion test facilities.," *Wear,* vol. 271, no. 9–10, pp. 2625-2631, 2011.

[15] "Smoothed particle hydrodynamics," [Online]. Available: https://abaqus-docs.mit.edu/2017/English/SIMACAEANLRefMap/simaanl-c-sphanalysis.htm.

[16] R. DALRYMPLE and B. ROGERS, *Modelling Tsunami Waves using Smoothed Particle Hydrodynamics (SPH) - Presentation,* Department of Civil Engineering, Johns Hopkins University.

[17] D. Spear, A. Palazotto and R. Kemnitz, "Modeling and Simulation Techniques Used in High Strain Rate Projectile Impact," *Mathematics,* vol. 9, no. 274, 2021.

[18] R. Wagner, "ABAQUS Tutorial: How to model graded material (GM) and functionally graded material (FGM) In ABAQUS CAE ?," 10 2020. [Online]. Available: https://www.youtube.com/watch?v=muoL_nmWcew&ab_channel=Dr.-Ing.RonaldWagner.

[19] "Haliade-X offshore wind turbine," GE, [Online]. Available: https://www.ge.com/renewableenergy/wind-energy/offshore-wind/haliade-x-offshore-turbine.

[20] R. Herring, K. Dyer, F. Martin and C. Ward, "The increasing importance of leading edge erosion and a review of existing protection solutions," *Renewable and Sustainable Energy Reviews,* vol. 115, 2019.

[21] University of Michigan, *Wind Energy Factsheet,* Pub. No. CSS07-09., 2020.

APPENDIX A

While developing the standard model, many iterations of the droplet-structure interface were modeled as shown in the following images. While optimizing the mesh for better resolution of the stress field was done, understanding how the parameters affected the stress field was important, such as how did the contact pressure vary when the mesh density or number of particles were increased. Optimizing the dimensions to accommodate the critical portions of the stress field was important as well, especially when considering a discrete interface. Therefore, iterations of a selected mesh were carried out for varying LEP and substrate thicknesses.

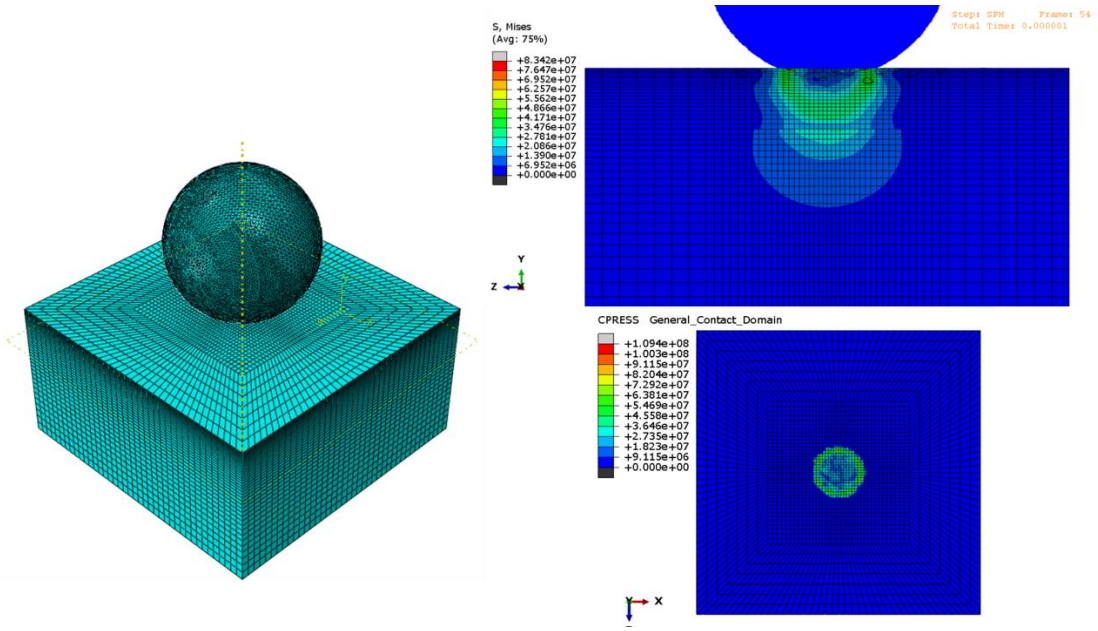

Figure 47. NM#1 showing Mesh assembly (Left), stress field (Right Top) and contact pressure (Right Bottom) for ABS LEP (0.2mm) and epoxy substrate (0.25mm).

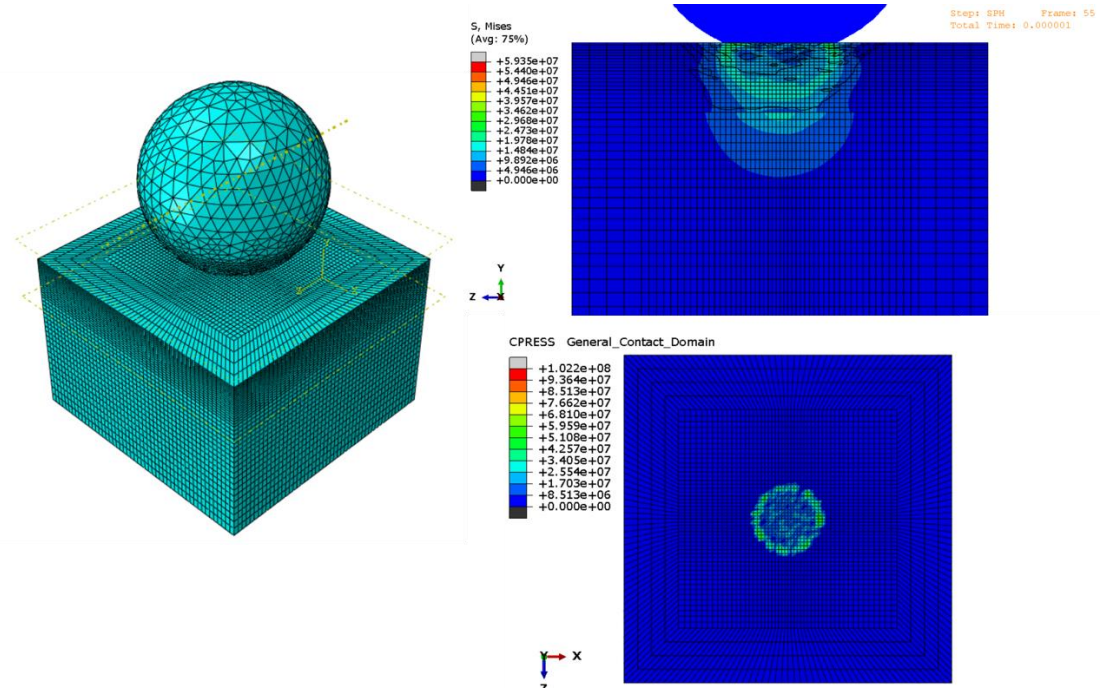

Figure 48. NM#2 showing Mesh assembly (Left), stress field (Right Top) and contact pressure (Right Bottom) for ABS LEP (0.2mm) and epoxy substrate (0.5mm).

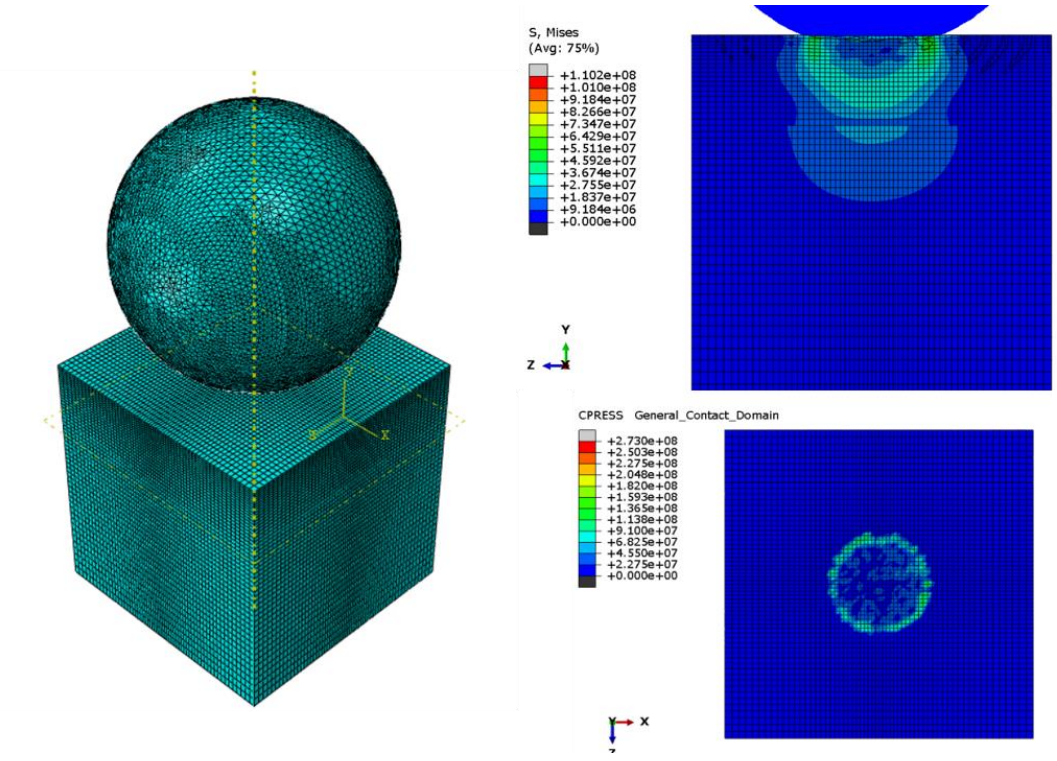

Figure 49. NM#3 showing Mesh assembly (Left), stress field (Right Top) and contact pressure (Right Bottom) for ABS LEP (0.2mm) and epoxy substrate (0.75mm).

APPENDIX B

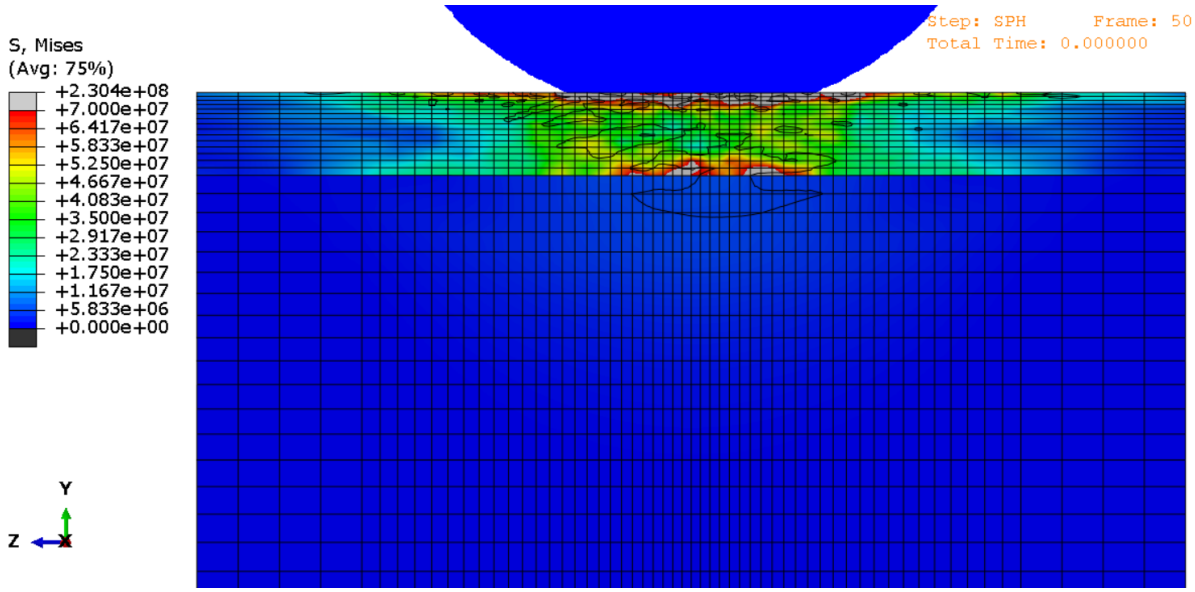

Figure 50. Von Mises stress field for the 0.25mm LEP, AL 3004,O.

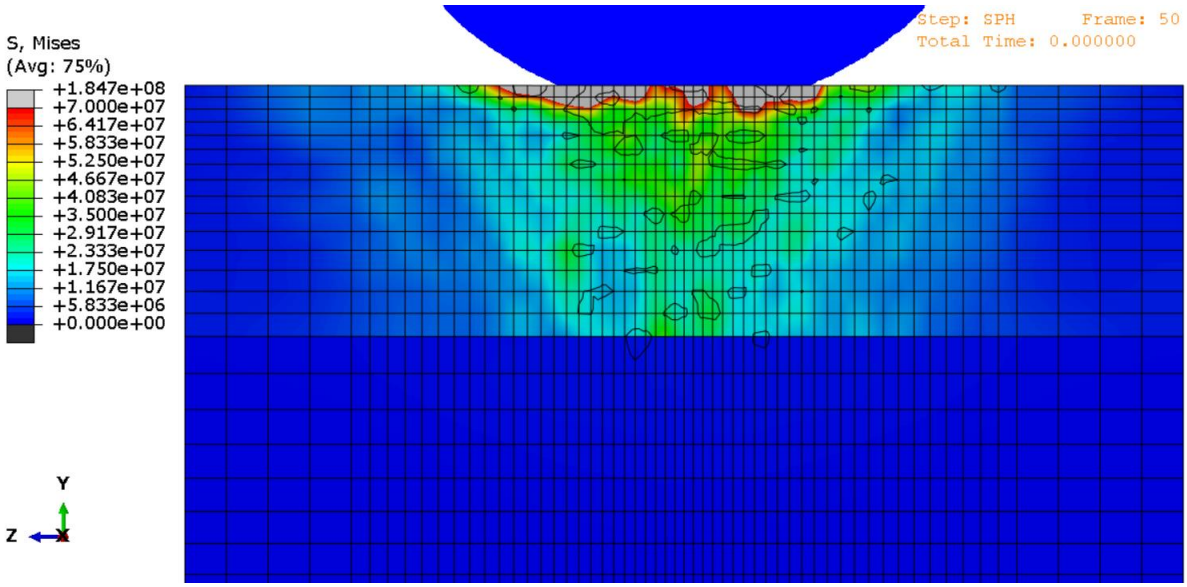

Figure 51. Von Mises stress field for the 0.75mm LEP, AL 3004,O.

The design guidelines derived suggest stiff materials would have superficial stresses and require thinner LEP's. Simulating the same for aluminium 3004, O indicates this to be the case as can be seen in the above images. The properties of AL 3004, O studied are as follows: Young's Modulus – 70 GPa, Density – 2700 Kg/m^3 and poisson's ratio – 0.34. This LEP shields the epoxy substrate effectively against droplet impact. However, here the LEP and substrate are assumed to be perfectly bonded. Therefore, it is recommended to analyze the same while considering an adhesive layer to obtain better resolution results, especially at the LEP-substrate interface considering the new adhesive layer.